Study on The Effects of Band Overload on Fatigue crack growth retardation

By

Mohammed Zuberuddin

NIT Rourkela

Rourkela

A thesis submitted for the award of Master of Technology in Mechanical Engineering

May-2009

Study on The Effects of Band Overload on Fatigue crack growth retardation

A thesis submitted in partial fulfillment of the requirements for the award of Master of Technology in Machine Design and Analysis

BY

Mohammed Zuberuddin

20714010

Under the guidance of

Dr.P.K.Ray

&

Dr. B.B.Verma

Department of Mechanical Engineering

NIT Rourkela

Rourkela

2009

Abstract

Most load bearing structural components are subjected to variable amplitude loading (VAL) rather than constant amplitude loading (CAL) during their service life. The simplest type of VAL is the occurrence of high peak loads interspersed in constant amplitude loading (CAL) history. Typical examples where this type of load interaction occurs are airplane flying under gust spectrum, ships and offshore structures coming under high loads during certain period of time etc. Overload-induced retardation has a significant effect on fatigue crack growth as it enhances the life of the structure. Therefore, it is essential to have a reliable estimate of life of structural components under such types of loading conditions.

The understanding of the effects of overloads on fatigue crack propagation in materials like the alloy Al 2024 used for airframe structures is important to ensure the reliability of the structure. Although various theories available describing the mechanism of crack retardation due to an overload, no model exists that can predict the post-overload life of a specimen subjected to continuous multiple overloads. Overloads are known to retard crack growth, while underloads accelerate crack growth relative to the background rate. These interactions, which are highly dependent upon the loading sequence, make the prediction of fatigue life under variable amplitude loading more complex than under constant amplitude loading.

When overloads are applied periodically, interaction between overloads becomes possible and retardation is enhanced. Certainly, too closely spaced overloads lead to acceleration rather than retardation since crack jump at each overload greatly exceeds the retardation in the subsequent few baseline cycles.

In the present work experiments were performed in *Instron*-8502 machine with a 250 kN load cell capacity. All tests were conducted in air and at room temperature. Tests were performed to investigate the effect of multiple consecutive overload cycles on constant amplitude fatigue crack propagation rate. For this purpose constant amplitude fatigue tests were carried out and overload was applied at an a/w ratio of 0.4 in all specimens, following which the same constant amplitude tests were continued. The overload ratio was maintained at 1.9 in all cases and the number of overload cycles applied was 1, 2, 5, 10 and 100. From experimental data it has

been observed that a single spike overload (1 cycle) gives maximum retardation and the retardation effect decreases with the increase in number of overload cycles. The number of delay cycles (N_D) and the retarded crack length (a_D) were obtained for all the above cases. The values of both these parameters decreased with increase in number of overload cycles. Finally a model has been developed to predict the post-overload life of a specimen. The model was developed with experimental data of 1, 2, 5 and 100 overload cycles and was verified by comparing predicted data and experimental data for 10 overload cycles.

The fractured surfaces of the test specimens were examined under SEM in order to investigate the nature of crack growth under different overload cycles. Fractogrpahs show that presence of micro voids and secondary cracks in the tear zone. This suggests development of a highly strained zone on application of overload cycles. It may be recalled that the extent of retardation reduces on application of multiple overload cycles. The overload tear zones are measured in different cases which show a maximum in case of 100 cycles. The width of the tear zones are nearly same for specimens subjected to overload cycles 2, 5 and 10. This suggests significant stress relaxation on application of large number of overload cycles. Thus the reduction in magnitude of retardation in case of multiple overloading may be due to stress relaxation and it becomes significant for large number of overload cycles.

List of figures

List of tables

Nomenclature

K	Stress intensity factor
K_{max}	Maximum stress intensity factor in a cycle
K_{min}	Minimum stress intensity factor in a cycle
ΔK	Change in Stress intensity factor in a cycle
σ_{ij}	Stress in ij plane
R	Size of plastic zone
v	Material constant
$d(a)/dN$	Crack growth rate
C &m	Paris material constant
σ_o	Stress at crack opening
σ_{max}	Maximum stress in a cycle
ΔK_{eff}	K_{max}-$K_{opening}$
a_d	Retardation in crack length
N_d	Retardation in number of cycle
A	Crack length
R^{OL}, *or O.L.R*	Overload ratio
F_g	Geometric correction factor for specimen
ΔP	Change in load in a cycle
K_{IC}	Plastic strain fracture toughness
E	Young's Modulus
σ_y	Yield strength of material
M	Specific growth rate
N	Number of cycles
A', B', C' & D'	Material constants in the 'Exponential Model'

Chapter -1

Introduction

1. Introduction:

Fatigue in metals can be defined as failure of a member due to the application of repeated and or fluctuating loads which are far less than that of static strength of the member.

Failure of member under fatigue loading can be classified into five steps based on crack propagation as mentioned below.

1. Crack nucleation caused by sub structural and micro structural changes.
2. The creation of microscopic cracks
3. Formation of dominant crack from the movement of dislocations and slip bands which eventually lead to cat strophic failure.
4. Stable propagation of dominant crack so produced.
5. Structural instability and complete failure of member.

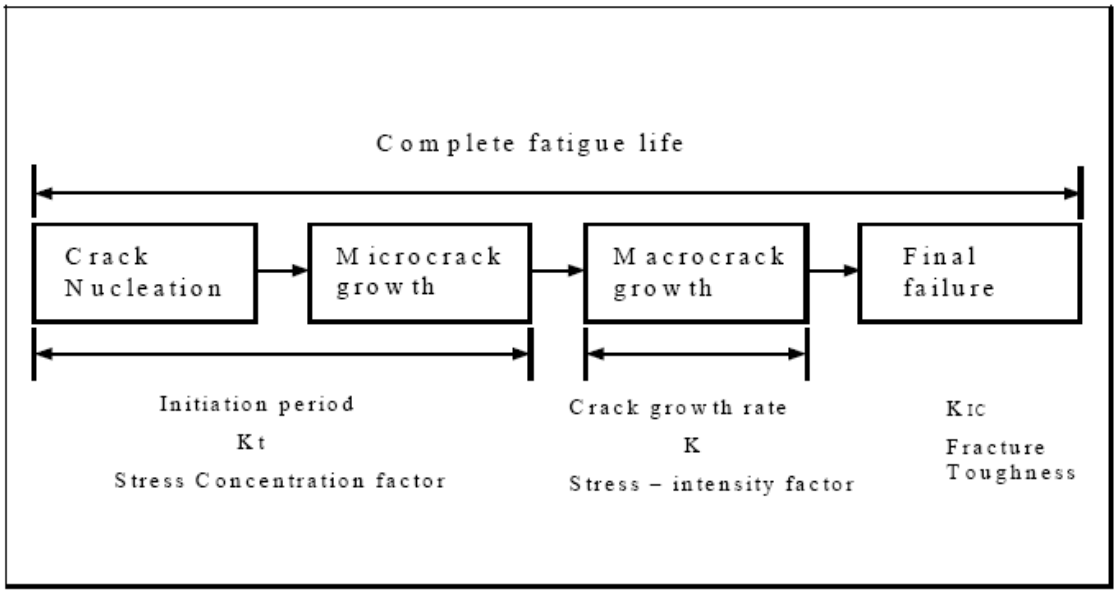

Figure 1.1 Different stages of fatigue crack growth

Total fatigue life of a component is defined as number of cycles or time to induce fatigue damage and to initiate a dominant fatigue flaw which propagates until final failure. As mentioned above load required to fail a component under cyclic loading is far less than

that of load required for static loading. This phenomenon of decreased loading that is required for failure the component was first studied by Bauschinger and the corresponding effect is known as Bauschinger effect as described below.

According to Bauschinger's effect if a material is subjected to forward plastic deformation in tension or compression and afterwards if the direction of application of load is changed then the material will yield at lower loads than the load required for forward plastic deformation. So during the application of cyclic loading the load requirement will gradually decreases and may reach even less than that of operating cyclic loading because of which the material will fail. Many aluminum alloys containing non-sharable strengthening properties are stretched prior to temper treatments to relieve thermal residual stresses. Since many of these materials exhibits Bauschinger effects they will exhibit low flow stresses if stretching direction is reversed.

Due to the decreased flow stress or due to damage caused by cyclic strain the flaws or micro structural irregularities will cause to initiate the fatigue crack. For example in case of Aluminum alloys, constituent particles such as the S-phase (Al_1CuMg) and ß-phase (Al_7Cu_1Fe) provide sites for fatigue crack nucleation [1]. In case of Al-1014 T4 alloys crack nucleation is initiated in particle matrix where there is a deboning due to cyclic damage. Or it may sometimes initiates along slip bands [3].

1.1.1 **Microscopic stages of crack growth**

On further application of cyclic loading the dislocations and irregularities that were present in the component will increase their severities in the vicinity of nucleated crack which finally leads to the formation of a dominant crack. The crack propagation due to the application of cyclic loading can be divided into two stages as shown in fig 1.2.

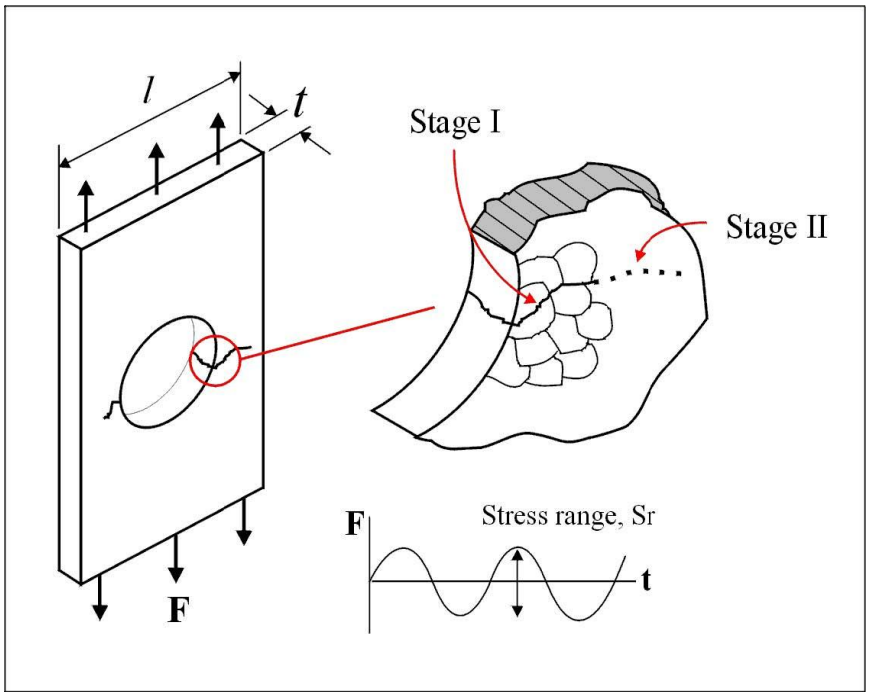

Figure 1.2 Illustration of stages of fatigue crack growth [1]

1.1.1 *Stage I crack growth*

The zigzag crack path that has been formed due to single shear of slip planes is termed as stage I crack propagation. In ductile solids, cyclic crack growth can be visualized as a process of intense localized deformation which tends to creation of newer crack surfaces. The direction of propagation of crack will be approximately 45^0 to the direction of load application. It will propagate for two to three grain boundaries.

1.1.1 *Stage II crack growth*

As crack propagates the crack tip compromises of many grains. Because of this simultaneous slip planes will develop which will lead to *stage II* crack propagation. In single crystals the transformation of *stage I* to *stage II* causes to the formation of dislocation cell structures and the breakdown of PSB's at the crack tip.

During *stage II* crack propagation the direction of crack growth will be almost perpendicular to the direction of application of load. The fracture surfaces created by stage II crack propagation is generally characterized by striations. For certain values of

imposed cyclic loads in Paris regime of fatigue crack advance, it has been found that the spacing between adjacent striations correlates with experimentally measured average crack growth rate.

Different mechanisms were proposed to explain the *stage II* fatigue crack growth. One among them is Plastic blunting mechanism proposed by Laird [4]. In this mechanism the crack extension is supposed to be occurred due to plastic blunting of crack tip. This model can be applied to almost all ductile materials. Another mechanism is based on strain hardening in the formation of duplex slip bands. Work hardening in primary slip will increases crack resistance which let the crack to find another nearby slip plane which will have less resistance. Thus crack will now propagate on second plane. Kinematic irreversibility of cyclic slip causes a net crack growth in a planer fashion along the line of intersection of two planes.

1.1. 2 **Stresses at crack tip and influence of ΔK**

For linear elastic materials Irwin [5] suggested describing the stresses in the vicinity of the crack by stress intensity factors. There are basically three types of stress intensity factors describing the deformation modes as shown in fig 1.3. The superimposition of these three modes will give general crack propagation known as mixed mode.

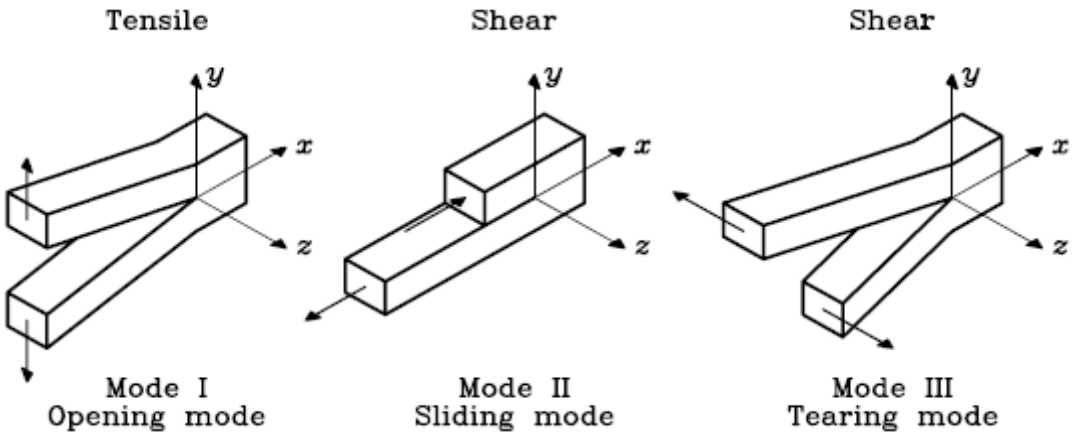

Figure 1.3 Modes of cracking

Mode I: In this the direction of application of load is perpendicular to direction of crack propagation. This is also known as opening mode and is most predominant in most of engineering applications.

Mode II: In this the direction of application of load will be in same direction of crack propagation which is also known as sliding mode.

Mode III: Tearing mode is caused by out of plane shear.

1.1.3 Different regimes in crack growth

Current theoretical and experimental linear elastic approaches tries to describe the stable and unstable crack growth by a crack propagation rate which can be defined as incremental crack growth d*a* divided by increment in number of load cycles d*N*. This fatigue crack growth rate can be correlated with stress intensity factor according to Paris law given by $\frac{da}{dN} = C(\Delta K)^{v}$ where *C* and *v* are material constants and $\Delta K = K_{max} - K_{min}$. If a graph is drawn between $\log\left(\frac{da}{dN}\right)$ and log (ΔK) it will be as shown in fig 1.4. This figure can be divided in to three regimes.

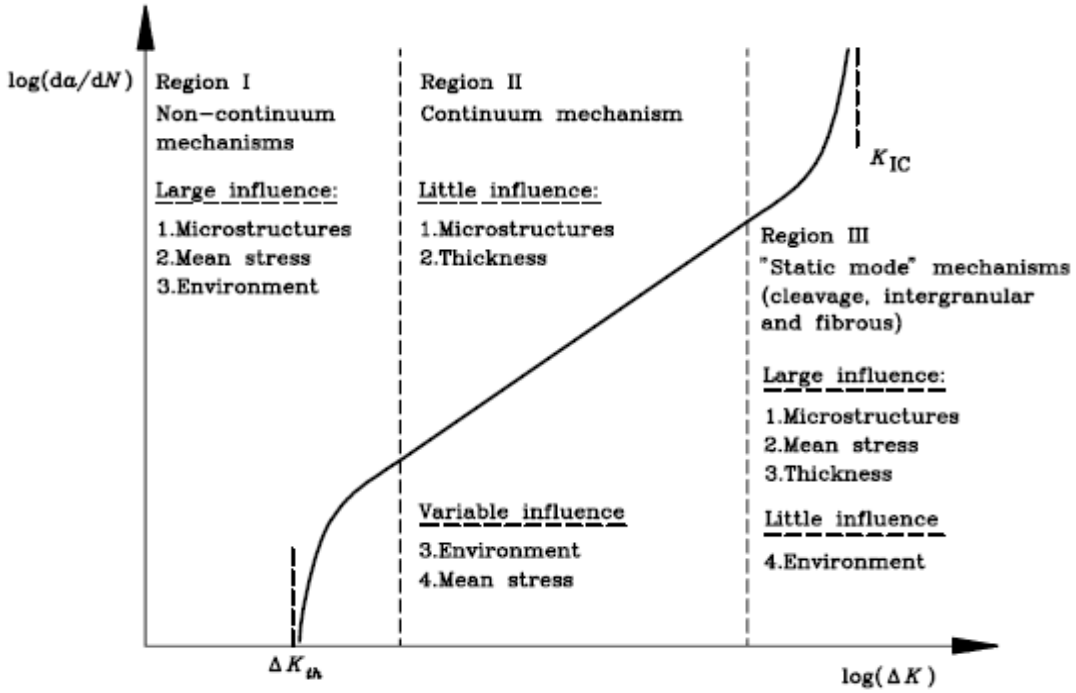

Figure 1.4 Different regimes of crack growth.

Region I: This region is characterized by an increase in $\log\left(\frac{da}{d\mathrm{N}}\right)$ asymptotically with log (ΔK). Crack can't be initiated until and unless ΔK reaches certain threshold value known as ΔK_{th}.Below this the increase in da/dN is very low that can't be measured experimentally. This regime is generally contributed by crack nucleation and early growth state. Above threshold da/dN will increase in a steep manner.

Region II: It is also called as Paris regime in which there is a linear variation of $\log\left(\frac{da}{d\mathrm{N}}\right)$ vs. log (ΔK). This region is characterized by stable crack growth.

Region III: This region is characterized by rapid crack growth rates. And the maximum stress intensity factor of the cycle reaches to fracture toughness K_{IC} of material.

1.1.4 **Effective ΔK and crack closure**

Crack extension can be take place if the material at crack tip has reached max permissible plastic strain. The amount of crack extension can be measured with Crack Opening Displacement (COD). This concept is introduced by Wells [7].

According to linear fracture mechanics, crack faces must be opened immediately after the application of tensile load and has to close during unloading as indicated by line II in fig 1.5. But for the materials with less fracture toughness when the material is stressed elastically under tension, the change of the applied stress from σ_o to σ_{max} as indicated by curve I. Curve I can be divided in to two parts a linear variation of COD and applied stress and the curve with decreasing slope from zero stress to σ_o. For the values of stress that are less than that of σ_0 crack faces will be remain in contact and are partially opened.

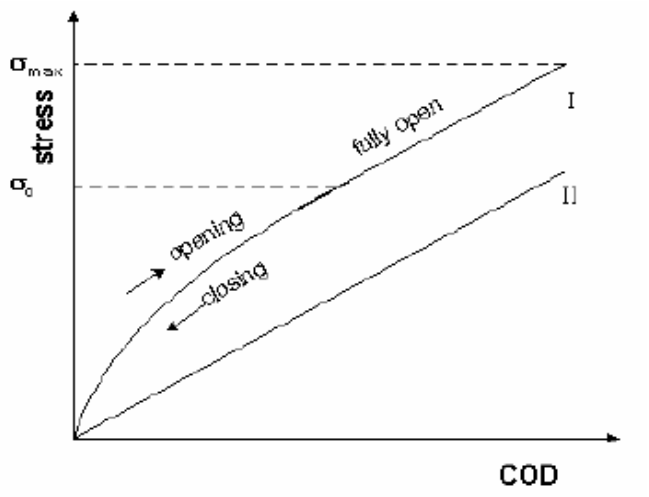

Figure 1.5 I. indicates with crack closure and II indicates without crack closure

Elber first observed that fatigue cracks can close even during tension-tension far field loading [8]. He argued that a zone of residual tensile deformation is left in the wake of a fatigue crack tip. The deformed material causes contact between the fracture surface of the fatigue crack and results in a reduction of the applied amplitude ΔK, so that only a reduced part of it contributes to crack propagation. This mechanism is known as plasticity induced-closure. But, it has been found that there are some additional closure

mechanisms like roughness induced-closure [9] and oxide induced-closure [10, 11], which can cause premature contact of the fatigue crack surfaces.

Elber argued that only the stress range from σ_o to σ_{max} is responsible for the crack propagation as shown in fig 1.6. So the effective stress range will be $\Delta\sigma_{eff} = \sigma_{max} - \sigma_o$ and corresponding stress intensity factor will be modified to $\Delta K_{eff} = K_{max} - K_o$. Thus Paris law will take a form of $\frac{da}{dN} = C(K_{eff})^v$

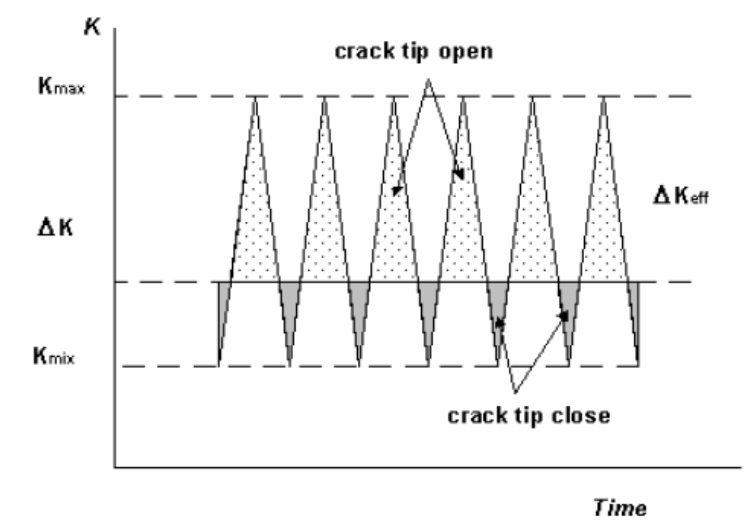

Figure 1.6 Crack tip behavior during cyclic loading with closure effect

In recent years Sadananda and Vasudevan [6] reported that closure occurring behind the crack tip has limited effect on the damage process that takes place in front of the crack.

1.2. Factors Affecting the Rate of Fatigue Crack Growth:

In this section we investigate and explain conceptually the effect of the following parameters on fatigue crack growth rate:

1. Stress or Strain Range
2. Mean Stress
3. Surface Finish and Quality
4. Surface Treatments
5. Sequence effects
6. Overload effects

We see that Stress or Strain range has the most important influence.

1.2.1 Stress or Strain Range:

From the previous description we notice that in both stage I and stage II growth, crack development arises through plastic shear strain on a microscopic scale. Consider, therefore, the plastic shear strain forming along the stage I slip planes or at the tip of a stage II crack as a result of the nominal stress time history shown in Figure 1.7

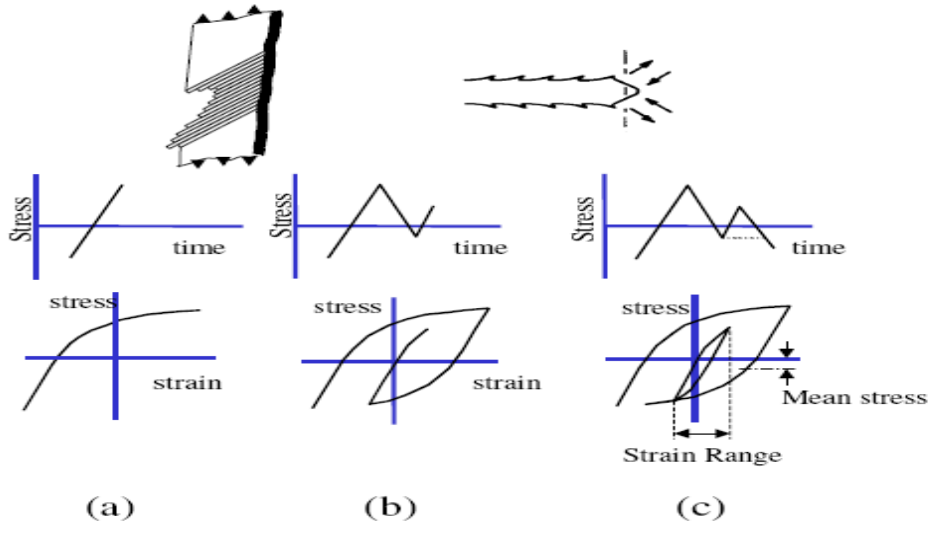

Figure1.7 Elastic-plastic stress and strain along slip plane and at the root of a crack

In Figure a, we see the nominal stress rise with time. On a microscopic level, in the presence of a crack or pre-existing defect, the stress and strain become plastic and can be plotted in the stress vs. strain diagram shown. Fig.1.7 now shows what happens when the nominal stress is reduced and then raised again by a smaller amount.

Again the local stress vs. strain can be plotted showing the effect of local yielding. Finally Fig. 1.7 shows another reduction in the nominal stress. From the stress vs. strain plot we now see the formation of a hysteresis loop. A loop in the stress vs. strain plot indicates release of strain energy where the total energy released is equal to the area of the loop. Essentially we have released a quantity of shear strain energy and this has been expended in sliding the slip planes or advancing the stage II crack.

From this illustration we therefore see that a 'quantum' of shear strain energy is released when the nominal stress is cycled into tension and then back again. Also, the larger the stress cycle, the greater the energy released.

1.2.2 Mean Stress:

The mean stress (or residual stress) will also affect the rate of fatigue damage. Viewed conceptually, if a mean tensile stress is applied to a stage II crack then the crack is being forced open and any stress cycles applied will therefore have a more pronounced affect. Conversely, if a mean compressive stress is applied then the crack will be forced shut and any stress cycle would first of all have to overcome the pre compression before any growth could ensue. A similar visualization can be made for a stage I crack. Here a mean compressive stress would increase the frictional resistance between the slip planes requiring more strain energy to propagate the crack. Conversely, a tensile mean stress would reduce the frictional resistance. Research into the effect of mean stress gave rise to the Haigh diagram shown in Figure 1.8. This plots the stress cycle amplitude vs. the mean stress for a number of tests whose fatigue lives were constant. It shows that for a certain tensile mean, the stress range would have to be reduced proportionally in Order to achieve the same fatigue life.

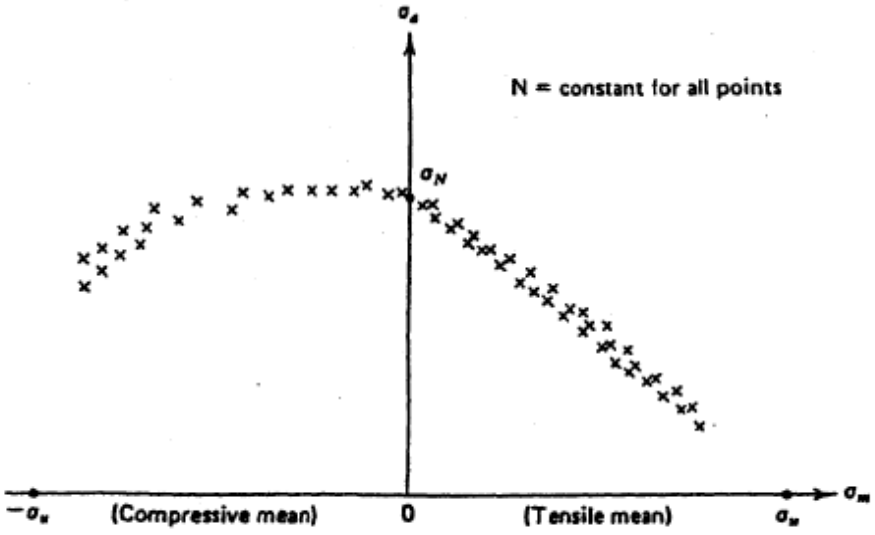

Figure 1.8 Haigh diagram showing the effect of mean stress on fatigue life

1.2.3 Surface finish:

Fatigue cracks usually initiate from a pre-existing defect at the surface of a component. Therefore the quality of the surface will greatly influence the chance of a crack initiating and hence evolving into a full stage II crack. Most material specimens tested have a high quality mirror polished finish and therefore achieve the best fatigue lives.

Surface finish has a more significant effect on the fatigue of components subjected to low amplitude stress cycles. The effect of surface finish can be modeled by multiplying the SN curve by the surface correction parameter at the endurance limit as shown in Figure 1.9. This has the effect of revolving the SN curve so low amplitude stress cycles show the greater effect for high cycles no data available. The amount of reduction is obtained from the empirical curves shown in Figure 1.9.

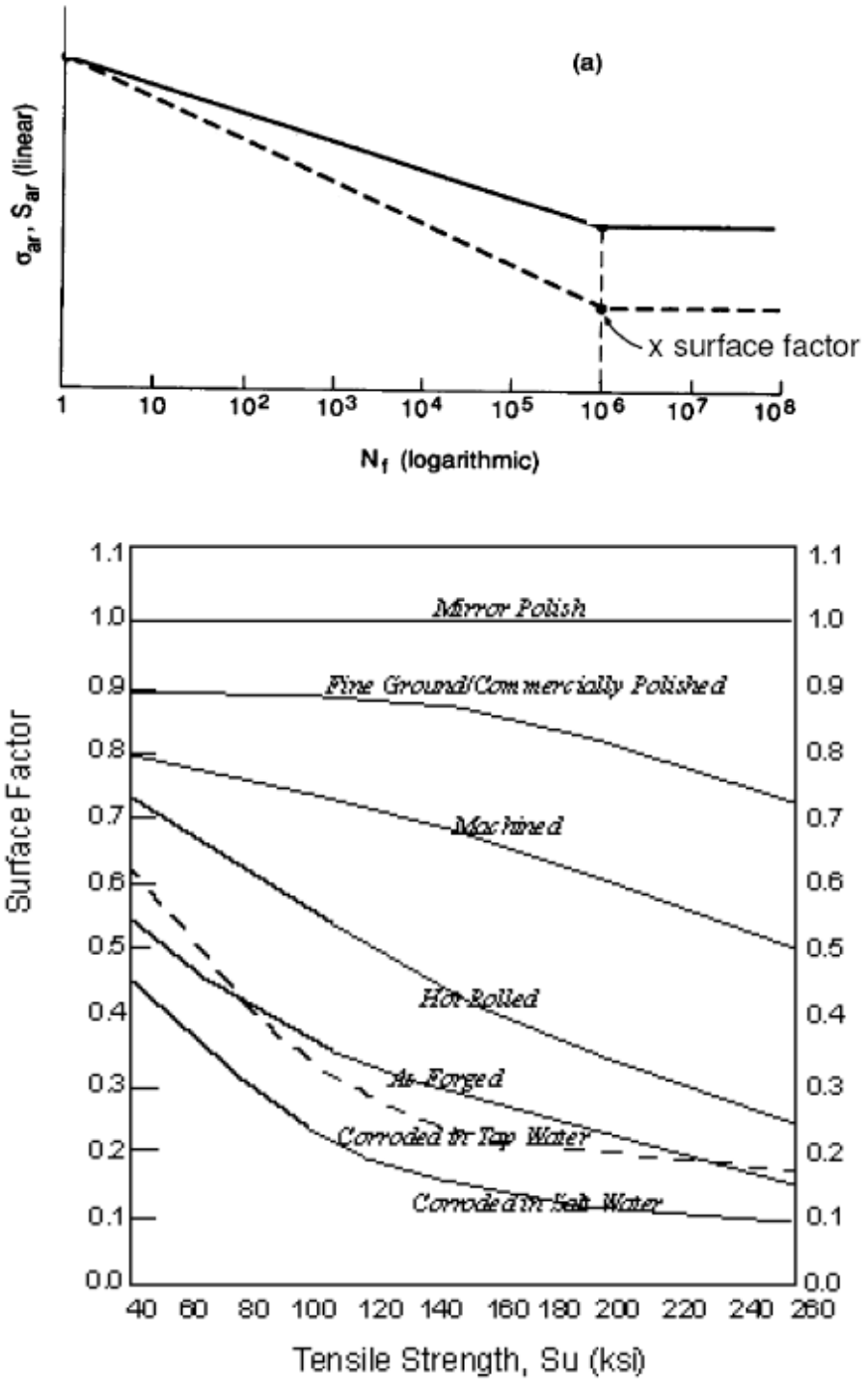

Figure 1.9 The effect of surface quality of fatigue life

1.2.4 Surface Treatments:

Surface treatments can be applied to improve the fatigue resistance of a component. These usually work by inducing a residual compressive stress at the surface. Figure 1.10 illustrates this effect by showing the stress distribution through a bar subjected an oscillating bending moment. Under low amplitude cycles the stresses at the surface are significantly lower or even remain compressive. Therefore the fatigue life is greatly improved. We note, however, that this effect is only true for components subjected to low amplitude stress cycles not for high cycles. If large amplitude cycles were applied then these would start to overcome the pre-compression and therefore the beneficial effect would soon be lost. In conclusion, surface treatments can be used to improve the fatigue performance of a component subjected to low amplitude cycles but becomes less effective for those with high cyclic stresses.

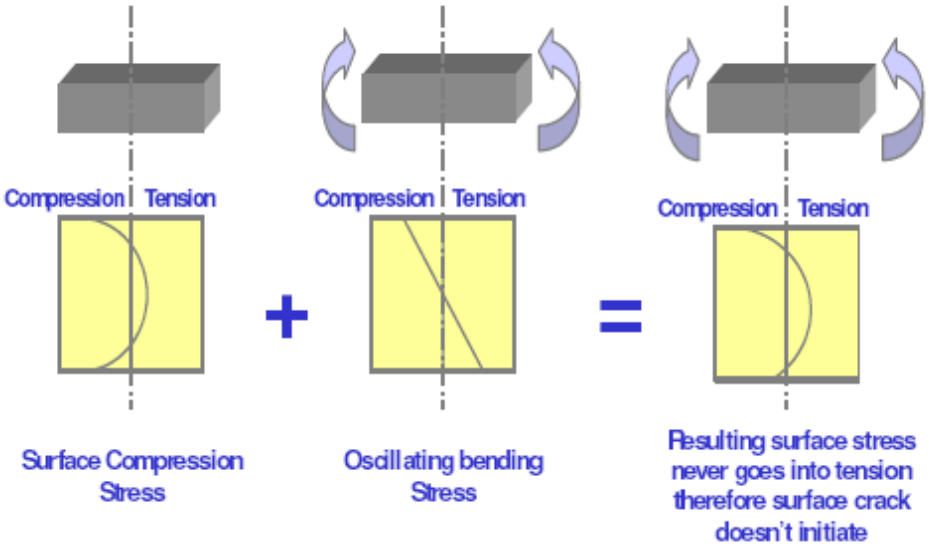

Figure 1.10 Illustration showing the effect of residual compression at the surface

1.2.5 Sequence effects:

The sequence in which cycles are ordered can influence the fatigue life. Consider the two time histories shown in Fig. 1.11. Both appear to consist of two cycles having the same range and mean stresses. However, if we plot the elastic-plastic response we see that the smaller cycle has a tensile mean in the first example and a compressive mean in the second. Therefore the first example will create more damage than the second. For most practical analyses, sequence effects are insignificant because the probability of one sequence occurring is equal to that of the other. However, it is worth bearing in mind when planning some simplified and idealized loading sequences.

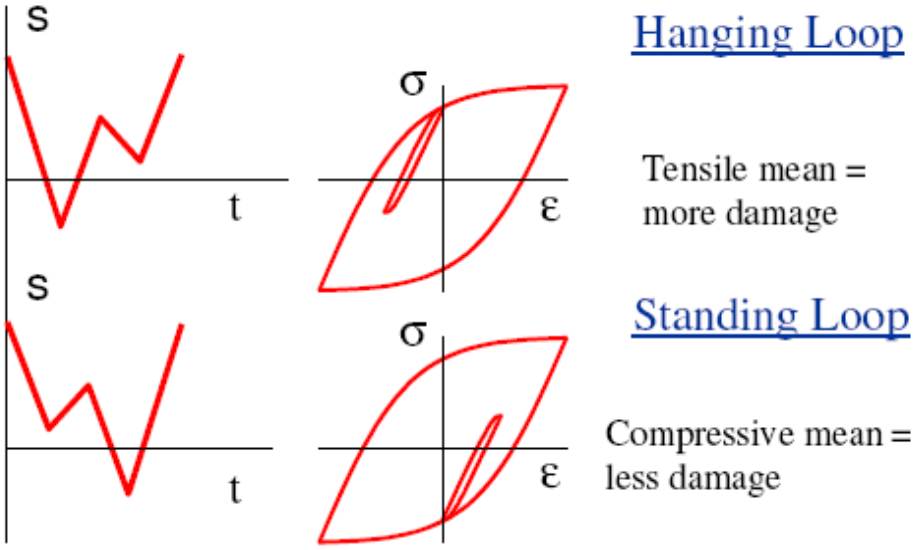

Figure 1.11 Illustration showing the effect of cycle sequence

1.2.6 Overload effects:

During stage II crack growth, tensile overloads can have a very positive effect on fatigue life. During the overload the high crack tip strain induces a large region of plastic deformation ahead of the crack.

This results in a plastic volumetric expansion that acts to close the crack. Any subsequent cycles have, first of all, to overcome the cracks pre-compression before causing damage. Therefore the crack growth rate is retarded. This is illustrated in Figure 1.12. This effect is known as crack retardation. The effect retards the crack growth rate until it has effectively propagated through the affected zone, after which it continues normally. In some circumstances a complete crack arrest can occur where the smaller cycles never get sufficiently large to overcome the volumetric pre-compression.

In an attempt to reinforce an understanding of this phenomenon, a popular fable was sited: when noticing a crack in the wing of an airliner you should instruct the pilot to roll the aircraft therefore inducing crack arrest. While this may be true you should also be aware that if you accidentally exceed the UTS you might have more immanent concerns than fatigue! While crack retardation can be used to good affect it has also been the cause of many serious fatigue oversights. In the early days of pressurised aircraft, for instance, overload tests were routinely carried out prior to fatigue testing. As the production aircraft did not undergo testing prior to flight they did not benefit from the overload and a number of fatal in-service failures occurred.

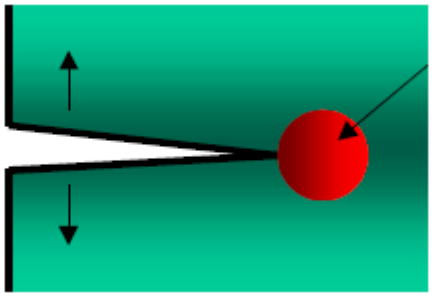

Figure 1.12 Illustration of plastic volumetric expansion at the crack tip during a tensile overload

Chapter -2

Literature review

2.1 Literature on crack retardation:

Crack is an unavoidable yet major source of failure in most of mechanical components. As mentioned in previous chapter if the stress intensity factor at the crack tip is crossed threshold value the crack propagation will be initiated and will leads to final failure. Once if the crack has crossed regime II i.e., stable crack growth and enters into regime III there will be rapid crack growth rate which will not leave even sufficient time for the component to get replaced (for components like gas turbines it will take years to gather to manufacture a new one and is also cost worthy). So all thing that can be done is to retard crack propagation before crossing regime II so that there will be sufficient time for a component get replaced and operating cost can be get minimized.

Till date different techniques were proposed to retard the crack growth rate. One method involves heating the whole cross-section and applying maximum load that would be experienced during the service [12]. This introduced a suitable compressive residual stress around the crack tip thus increases the crack tip resistance. But this will lead to general yield as temperature increases. Harrison [13] has proposed another technique to heat directly near the crack tip. But this requires precise heating and direct heating may cause damage to surface. More recently Ray [14] proposed to heat a spot ahead of crack tip to a sub critical temperature. One more old technique that is available for retardation is application of overload spike over normal operating cyclic loading.

During normal cyclic loading if an overload spike is applied as shown in fig 2.1 the crack growth rate is found to be decreased. During and after the application of overload spike following things can be observed.

- The ductile solid generally exhibits a temporary accelerated crack growth rate during and immediately after the application of overload
- In post overload regime, for same amount of base line stress intensity factor ΔK_B there will be a deceleration in crack growth rate.

- After reaching to a minimum, crack growth rate will again start increasing and finally after certain delayed number of cycles it will again reaches to base line crack growth rate.

The crack length at which the crack growth rate reaches minimum is generally known as delayed distance a_d.

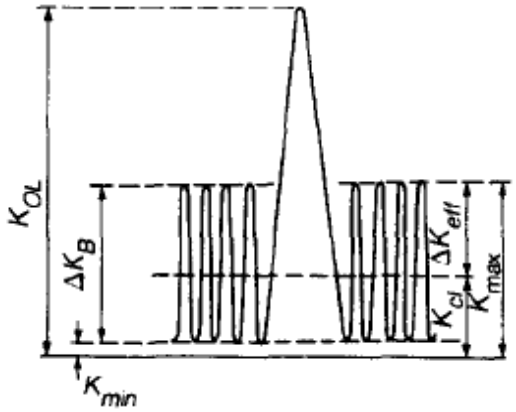

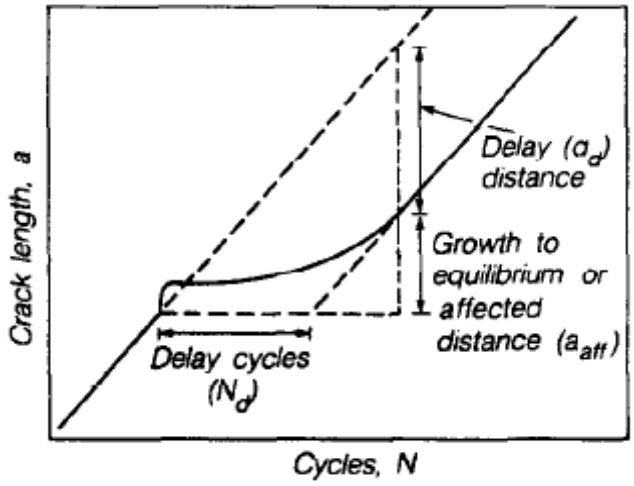

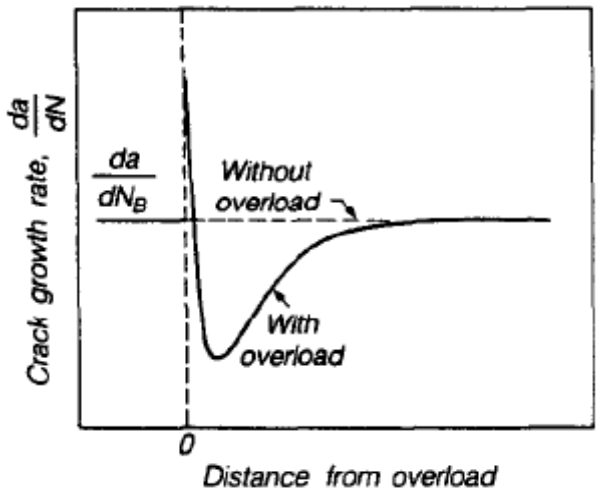

Figure 2.1 Effect of overload [13]

2.1.1. Mechanisms contributing to retardation

The various arguments which have been proposed over the years to rationalize post-overload fatigue fracture in ductile alloys can be classified into following groups.

A. Plasticity induced crack closure.

B. Crack tip blunting.

C. Residual compressive stresses.

D. Deflections or bifurcation of the crack.

2.1.1.1.Plasticity induced crack closure:

Elber argued that plasticity induced crack closure can account for the retardation caused by overloads. Application of overload spike produces a plastically stretched zone in the wake of crack tip. This causes contacting of fatigue crack facets during its propagation which finally leads to retardation of its growth. Further Ward-Close [15] suggested that contact of crack facets causes a frictional resistance which produces the striations on the fractured surface. This reason has been proven by fractogrpahic analysis of Al alloys which shows significant striations on fractured surfaces.

During the application of constant amplitude loading at given base line stress concentration factor ΔK and crack growth rates will be constant and will be in equilibrium with its monotonic plastic zone. On application of overload severe shear bands will develop at crack tip. This will result in wider crack opening displacements and hence less closure will present immediately after the application of overload. Thus the crack will get accelerated.

Even though this mechanism can explain the reason for retardation but it can't give consistent reasons for some alloys. According this mechanism there will be a decrease in ΔK due to closure effect which decreases amount of retardation that is coming during post overload period. Many characteristic features such as change in mode of failure after the application of overload can't be explained with this mechanism.

2.1.1.2. Crack tip blunting:

Blunting means loss of sharp edge. Whenever a sharp crack tip is loaded until plastic deformation fundamentally two modes of deformations may takes place. The crack may propagate or it may emit dislocation. The sharp edge can propagate along any one of planes of maximum shear stress. The process of crack propagation by crack tip blunting can be explained through fig2.2 [5].

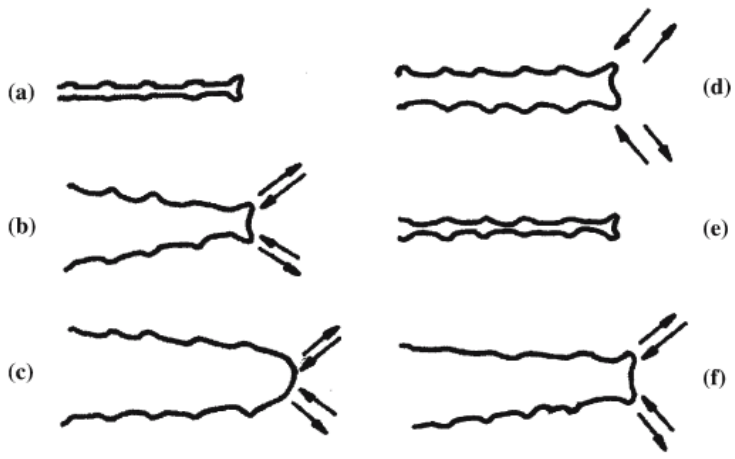

Figure 2.2 Crack tip blunting [5]

The initial (zero) load corresponds to a well developed Stage II crack with the fracture surface exhibiting striations (a). As the tensile load is applied, the metal yields plastically due to high stress concentration. This plastic deformation is highly concentrated in the slip zones along the planes of maximum shear stress (b). When the load is further increased, the slip zones at the tip broaden and the crack tip blunts to a semicircular configuration. The crack tip thus is effectively shifted (c). If the far-field stress is reversed, the crack tip re-sharpens by buckling and folding of the new created surface into a double notch resulting in a striation formation (d) and (e). Since the closure of the crack during compression cannot fully negate the blunting and the attendant extension of the crack during the preceding tension load, net crack growth occurs during a fatigue cycle, leading to the formation of a striation with the striation spacing equal to the crack length increment.

Due to the application of overload the sharp edge of crack tip is get curved. This reduces severe stress concentration that would present at sharp edge of crack tip [16]. It is generally observed in polymeric materials such as poly carbonate. But this mechanism doesn't account for other crack growth mechanism such as corrosion, debris and damage evaluation etc. This is a purely ductile mechanism that can fit in Paris law according to which da/dN directly proportional to ΔK [17].

2.1.1.3. Residual compressive stress:

Reverse yielding of a fatigue crack loaded in cyclic tension produces residual compressive stresses. When a tensile overload is applied, the size of residual compression increases. It has been suggested that this compressive stresses can retard the crack propagation [12]. But this mechanism can't explain the delayed retardation that is coming during the application of overload. As the compressive zone size is larger immediate after the application of overload one should expect the instantaneous retardation or even crack arrest which is not the case.

2.1.1.4. Deflections or bifurcation of the crack:

In some engineering alloys with planar slip as primary fracture mechanism, and under plastic stress loading conditions, the application of overload will promotes the deflection of crack from nominal mode I crack growth plane [18]. Fig2.3 explains this

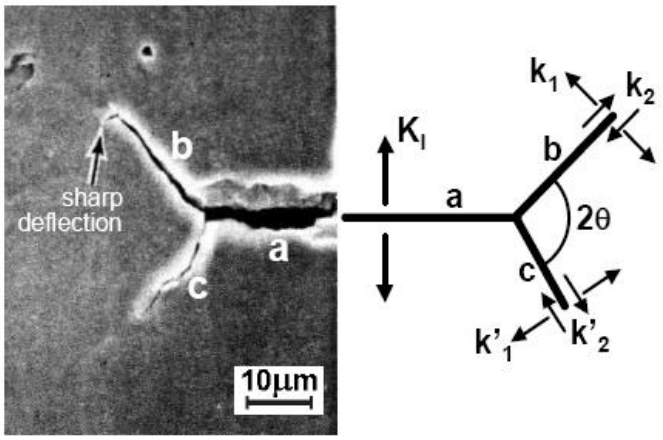

Figure 2.3 Crack branching [19]

The growth of the fatigue crack along a deflected path implies reduced crack propagation resistance away from the mode I growth plane. Thus there will be a temporary acceleration during the application of overload which was pointed by [19]. But later on due to branching of crack net effect stress intensity factor will be decreased which ultimately causes a reduction in crack growth rate. It is experimentally observed that very small deviation in crack lengths of b and c is sufficient to arrest smaller crack [18].

2.1.2. Factors affecting amount of retardation:

The amount of retardation that can be achieved by the application of overload depends on different factors like position of application of overload, amount of overload ratio, background ΔK, working environment etc.,

2.1.2.1. Effect of overload ratio

As amount of overload ratio increases the amount of retardation achieving also increases as shown in fig [2.4].

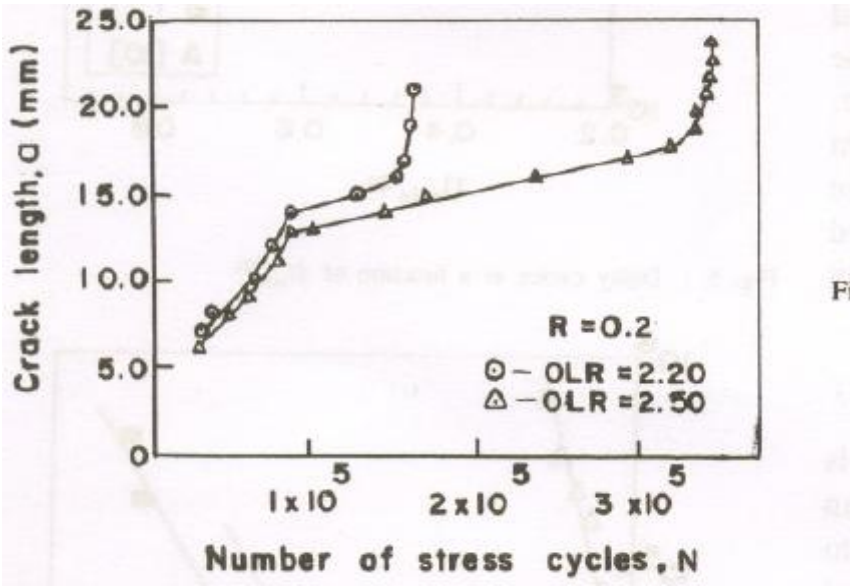

Figure 2.4 Variation of Fatigue life with overload ratio [18]

2.1.3. Models for predicting crack growth rate and amount of retardation

Based on above mentioned mechanisms a number of empirical models have been proposed to find fatigue life in case of variable amplitude loading. These models can be classified in to three main categories viz., the yield zone models [21-22], crack closure models [24-27] and strip yield models [28, 29]. In addition to those there are other retardation models [20, 21] based on damage accumulation and the strain energy release rate, but each model has its own capabilities and limitations as discussed in several literatures [21, 22].

2.2 Literature on band overloading:

In recent years, competition in the aerospace industry has increased pressure to reduce costs in all areas of aircraft design and manufacture. Aircraft manufacturers are looking to new materials and new processing methods to reduce cost and improve performance of their aircraft. Castings allow complex sub-assemblies to be redesigned into single components reducing tooling, inventory, labor, and materials costs. Although castings offer significant weight and cost savings to the aerospace industry, aircraft safety is of utmost importance where the study of both the static and dynamic mechanical behavior of cast materials is critical.

To ensure design safety, engineers need to be able to model or predict fatigue crack growth behavior accurately. Under constant amplitude loading, this is relatively simple. When transient or variable amplitude loading is introduced, however, fatigue crack growth modeling becomes more difficult. In order to accurately model transient crack growth behavior, several models have been proposed to account for the crack growth retardation or acceleration that is often observed. Of these, retardation models based on crack closure are quite common. Elber observed that crack faces came in contact before the specimen was completely unloaded and proposed that crack growth could occur only when the crack tip is fully open. This led to the concept that the effective stress intensity range, ΔKeff, was the driving force behind crack growth rather than the nominal stress intensity range ΔK. ΔKeff is defined as the difference between the maximum stress intensity, K_{max}, and the stress intensity required to open the crack, K_{op}. The crack closure concept has been incorporated into several fatigue crack growth life prediction codes and has been shown to model variable amplitude fatigue crack growth behavior reasonably well [30-33].

Service loads are mostly random in nature. It is well known that load fluctuations lead to fatigue crack propagation, the rate of which depends on the interaction of loads or stresses. Heavy opening loads on cracks cause large immediate incremental growth, but greatly disturb the crack tip parameters leading to retarded growth in the following cycles. The underlying mechanisms of this retardation need to be discovered to model crack growth effectively. There is substantial work done on various retardation mechanisms [34-35] but still one cannot start with these mechanisms and come up with a

quantitative prediction of growth. To have a starting point it helps to know the phenomenological behavior under various load combinations, particularly under extreme situations. Single overloads and maximum interaction between periodic or band overloads are such cases.

The former has been addressed previously by many authors [35-40] but the periodicity of overloads as to their optimum spacing to lead to maximum retardation is not emphasized enough. Single overload is characterized typically by the ratio of the overload to the maximum of the base loading which is called overload ratio.

The understanding of the effects of overloads on fatigue crack propagation in materials like the alloy Al 2024 used for airframe structures is important to ensure the reliability of aircrafts. Although the effect of different kinds of overloads on the crack propagation rate is well known there is a lack of a consistent theory describing the underlying mechanism affecting the propagating crack. Overload effects were explained on the basis of many mechanisms like plasticity-induced crack closure, local residual stresses, crack tip blunting and others reviewed by M. Skorupa [42]. The work performed in the last 40 years raises the question if the overload effect can be linked to one single mechanism or if the characteristic mechanism depends on factors like material, microstructure and environment. As a basis for reliable prediction models further investigations have to be done to improve the knowledge about overload effects and thereby improve the reliability of crack propagation prediction models. J. Schijve [43] emphasized the significance of fractography for the investigation of variable amplitude loading effects as an indispensable way for this purpose.

Retardation is mainly a surface phenomenon in aluminum alloys, i.e. plane stress regions are responsible for the major part of retardation. Machining surface layers, for example, after overload application eliminated retardation in 6061-T6 al-alloy [43]. Similarly, experiments on Ti-alloy showed a tightly closed crack within the plastic zone. But as the surface layers were polished away the closure effect (tightly closed crack faces) disappeared which was indicative of the minimal contribution of the plane strain region to retardation [43]. Crack closure does play a predominant role, but other mechanisms also contribute to retardation such as residual compressive stresses ahead of the crack tip, shear lip effects, strain hardening, etc., particularly for steel [42]. When overloads are applied periodically, interaction between overloads becomes possible and retardation is enhanced. Certainly, too closely spaced overloads lead to acceleration rather than retardation since crack jump at each overload greatly exceeds the retardation in the subsequent few baseline cycles. In cases of densely applied or remotely spaced overloads this interaction is trivial, but there is a large range in between where the enhanced retardation is worthwhile to study. For remotely applied overloads the crack growth is non uniform, reflecting intermittent crack advance; as interaction between overloads starts crack length change with number of cycles curve, on the macro scale, becomes a smooth line, similar to constant amplitude loading but of slower growth rate.

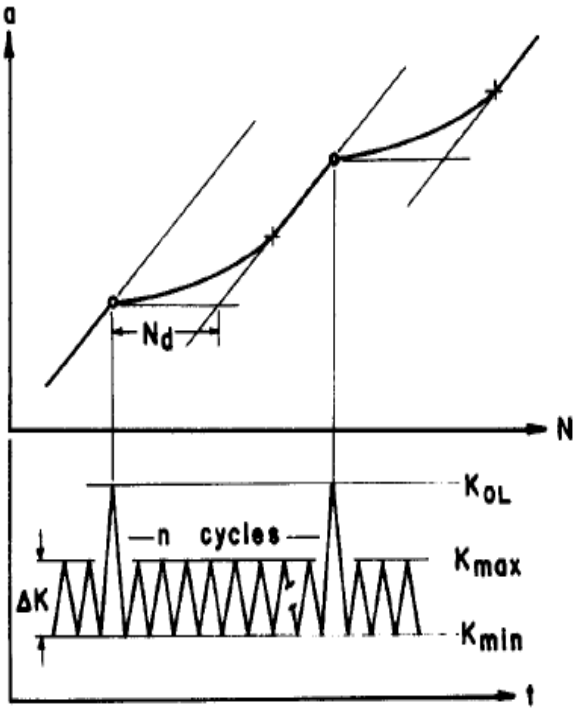

. A typical behavior of crack length as a function of number of cycles, at constant ΔK, which results from isolated overloads.

Figure.2.5 [43]

Crack growth in structures depends on the amplitude, stress ratio, and frequency of the load. Due to the random nature of variable loading, it is difficult to model all these influential parameters correctly. Overloads are known to retard crack growth, while underloads accelerate crack growth relative to the background rate. These interactions, which are highly dependent upon the loading sequence, make the prediction of fatigue life under variable amplitude loading more complex than under constant amplitude loading. Many models have been developed to predict the fatigue life of components subjected to variable amplitude loading [44–47]. The earliest of these are based on calculations of the yield zone size ahead of the crack tip and are still widely used. The Wheeler model [48] and Willenborg et al. model [49], for example, both fall into this category. Another category models based on the crack closure approach, which considers plastic deformation and crack face interaction in the wake of the crack, was subsequently proposed by Elber [50], have been used to model crack growth rates under variable amplitude loads [49–57]. More recent proposals include combinations of the Wheeler model with the Newman crack closure model [54] and model based on the strain energy

density factor [58]. However, due to the number and complexity of the mechanisms involved in this problem, no universal model exists yet.

Crack closure experiments on 6061-T6 Al-alloy for various bands of overloads [59]. These bands of overloads were applied after an interval of 10% CAL life from the beginning and after exhausting 50% CAL life. The sequence is almost constant amplitude loading with periodically inserted multiple overloads, which subsequently cause noticeable crack growth delay. After application of an overload band, the value of crack closure is increased in the case of the load being applied after exhausting 50% CAL life. This crack closure value is stabilized for the remaining periodically inserted overload bands. This" stabilized closure value is higher than the closure value at constant amplitude loading. When overload bands" were given from the beginning, crack closure was observed after 1 mm crack length. This closure value was stabilized and found higher than the closure value at constant amplitude loading. The life was increased in all three cases as compared to the CAL life of the specimen. This increase in life is due to a higher value of the crack opening load.

2.3 Problem formulation

From the literature gathered so far it can be found that enough work has been done on overload retardation at single overload at room temperature. A few investigators have studied the effect of multi overload cycles on crack growth retardation. However no serious attempt has been made to model and predict fatigue life in case of band overloading.

2.4 The objective:

- To study the effect of band overload application on fatigue crack growth behavior and fatigue life.
- To develop a model to predict *a*-*N* curve and hence fatigue life in case of band overload application.
- To study the mechanism of fatigue crack growth through fractogrpah under band overloading.

Chapter -3

Experimental

3.1 Specimen Material:

Aluminum alloys find extensive applications in transport industries, aerospace industries, and defense and for consumer durables due to their higher strength to weight ratio, corrosion resistance and high ductility. Aluminum alloy 2024 alone is used for conducting the tests, was procured from Virat Aluminum, Mumbai, Maharashtra, India in T3 heat-treated condition. Al 2024 T3 is widely used in aircraft industry owing to its high strength to weight ratio. Chemical composition of this alloy is given in Table 3.1. Mechanical properties of this alloy are given in Table 3.2.

Mats.	Al	Cu	Mg	Mn	Fe	Si	Zn	Cr	Others
Al-2024T3	90.7– 94.7%	3.8 – 4.9 %	1.2–1.8 %	0.3 – 0.9 %	0.5 %	0.5 %	0.25%	0.1%	0.15%

Table 3.1 Chemical composition of Al 2024 T3

Material	Tensile strength(σ_{ut}) *MPa*	Yield strength(σ_{ys}) *Mpa*	Young's modulus(*E*) *Mpa*	Poisson's ratio *(v)*	Plane Strain Fracture toughness(K_{IC}) $MPa\sqrt{m}$	Elongation
Al-2024T3	469	324	73,100	0.33	37.0	19 % in 12.7 *mm*

Table 3.2 Mechanical Properties of Al 202-T3

Single-edge notched, SEN specimen having a thickness of 6.48 mm were used for conducting the fatigue test. The specimens were made in the LT plane, with the loading aligned in the longitudinal direction. The detail geometry of the specimens is given in Fig 3.1.

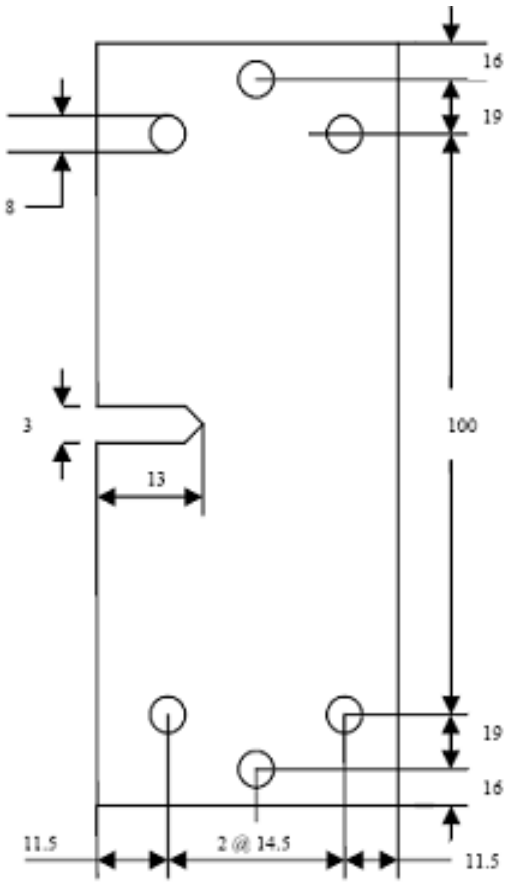

Figure 3.1 SEN Specimen Detailed geometry

3.2 EXPERIMENTAL PROCEDURE:

The experiments were performed in *Instron*-8502 machine with 250 kN load cell capacity. All tests were conducted in air and at room temperature. Both the surfaces of the test specimen were mirror polished and marked at every one mm interval in order to measure crack length by visual method.

The single edge cracked tension specimens have been used for fatigue test in the present investigation. For this purpose, specimens have been machined with their longitudinal axis parallel to the rolling direction of the sheet with width equal to 50mm .thickness equal to that of the supplied sheet 6.48 mm.

The specimens have been further given a flat notch of 13.5 using milling and then notch sharpened to a length of 14.3 using a fine jeweler's saw. The samples have been polished and graduated at an interval of 1mm.the dimensional detail of specimen is presented in Fig.

1. Precracking of the specimens was done up to an a/w ratio of 0.3 in the Mode I loading with a sinusoidal waveform using a Stress Ratio of 0.1. The crack length in the precracked samples were 15.3 mm. The sinusoidal loads were applied at a frequency of 6 Hz
2. The precracked specimen was subjected to constant amplitude loading cycles.
3. Crack monitoring was done optically using a low magnification microscope.
4. The following equation was used to determine stress intensity factor 'K' [60]

$$K = \mathrm{f}(g).\frac{F\sqrt{\pi a}}{wB} \qquad (3.1)$$

Where, $\mathrm{f}(g) = 1.12 - 0.231(a/w) + 10.55(a/w)^2 - 21.72(a/w)^3 + 30.39(a/w)^4$

a = crack length in mm

w = width of specimen=52mm

5. The fatigue crack was allowed to grow up to an *a*/*w* ratio of 0.4 at frequency of 6 Hz and subsequently subjected to multiple overload cycle at a load rate of 8 KN/min.

6. The specimens are to be subjected to Mode I overload having overload ratio 1.9.

$$R_{ol} = \frac{K_{ol}}{K^{B}_{max}} \tag{3.2}$$

Where, K^{B}_{max} is the maximum SIF for baseline test.

K_{ol} is the SIF at overload.

7. After application of the band overload, the specimens were subjected to Mode I constant amplitude load cycle at a frequency of 6 Hz.

3.3. **Procedure for the determination of crack growth rate**

3.3.1 By using exponential equation:

Earlier Mohanty et al. [61] used Exponential model to predict retardation parameters and fatigue life in 7020 T7 and 2024 T3 Al-alloys. The same form of equation has been used here with little modification to suit band overloading. The following are the procedural steps given by Mohanty et al. [61].

Based on the concept of exponential nature of crack growth, the crack length vs. number of cycles data have been fitted by an exponential equation of the form:

$$a_j = a_i e^{m_{ij}(N_j - N_i)} \tag{3.3}$$

Where, a_i and a_j = crack length in i^{th} step and j^{th} step in 'mm' respectively,

N_i and N_j = No. of cycles in i^{th} step and j^{th} step respectively,

m_{ij}= specific growth rate in the interval *i-j*,

i = No. of experimental steps,

And $j = i+1$

1. The exponent 'm_{ij}'in the above equation is an important controlling parameter. This is not a constant quantity and it depends on a number of factors like loading history and material properties. The specific growth rate 'm_{ij}' is derived by taking logarithm of equation (3.3) as follows:

$$m_{ij} = \frac{\ln\left(\frac{a_j}{a_i}\right)}{(N_j - N_i)} \tag{3.4}$$

2. The raw values of specific growth rate (m_{ij}) are calculated from experimental *a–N* data. These are fitted with corresponding crack lengths by a polynomial curve-fit.
3. For a better fit, crack lengths at small increments (0.05 mm in the present case) are tabulated and the corresponding values of *m* are obtained using polynomial equation.
4. The above values of specific crack growth rates are used to get the smoothened values of the number of cycles using the following equation:

$$N_j = \frac{\ln\left(\frac{a_j}{a_i}\right)}{m_{ij}} + N_i \tag{3.5}$$

5. The crack growth rates (d*a*/d*N*) are calculated directly from the above calculated values of '*N*' as follows:

$$\frac{da}{dN} = \frac{(a_j - a_i)}{(N_j - N_i)} \tag{3.6}$$

Chapter -4

Results and Discussion

4.1 Experimental results:

The crack length (a) as a function of stress cycles (N) has been presented in Fig.4.1. It is found that as the number of over load cycle increases amount of retardation decreases and for 1 overload cycle the retardation is maximum.

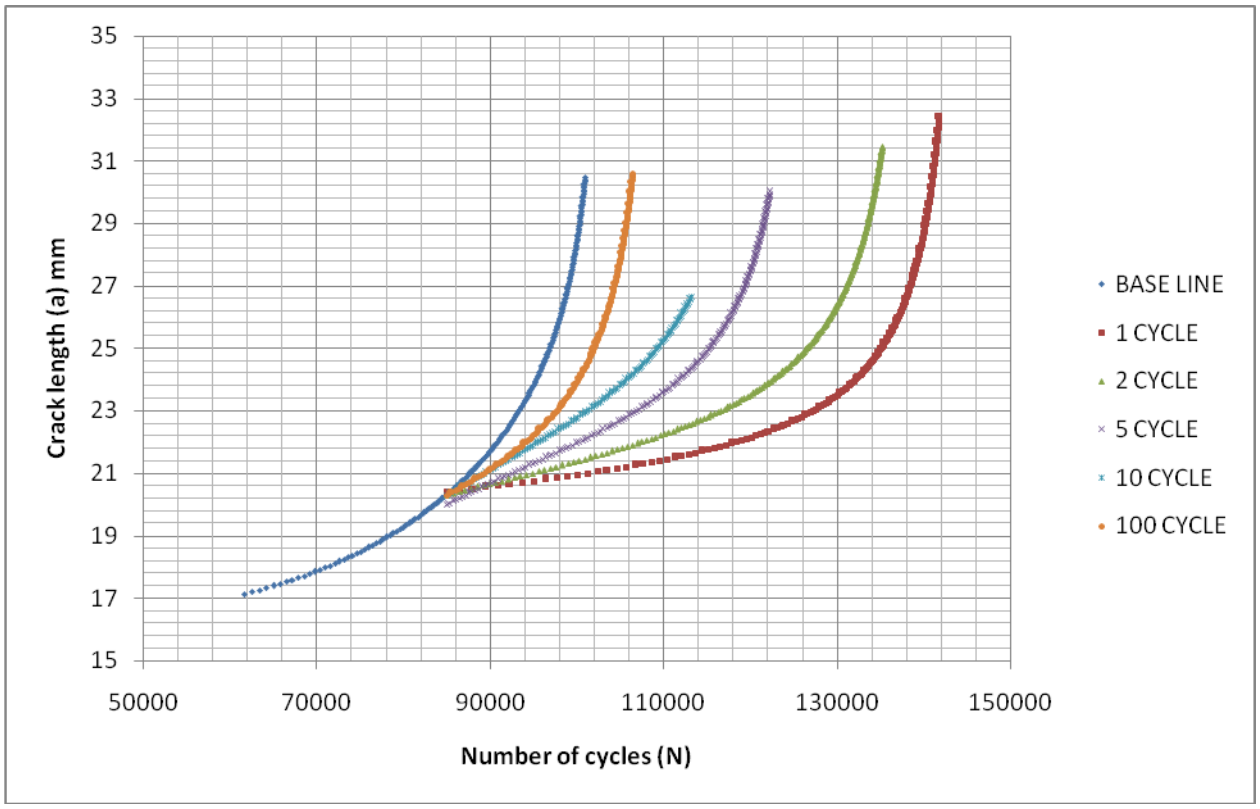

Figure 4.1 a ~ N for different overload cycles

The retardation parameters a_D and N_D have been calculated from the above figure and the values are presented in Table 4.1 below.

No. of overload cycles	a_D (mm)	N_D (No of cycles)
1	5.4	4800
2	4.1	4000
5	3.8	2800
10	3.2	1800
100	1.8	1000

Table 4.1 retarded zone length a_D ~ delay cycles N_D

It can be seen from Table No. 4.1 and Fig. 4.1 that the magnitude of retardation reduces on application of multiple overload cycles. Delay cycles n_D is 5.4 mm incase of application single overload cycle which has reduced to 1.8 mm when subjected to 100 overloaded cycles. This reduction in the magnitude of retardation may be linked with stress relaxation and reduction in magnitude of residual stresses which develops ahead of crack tip on overload application.

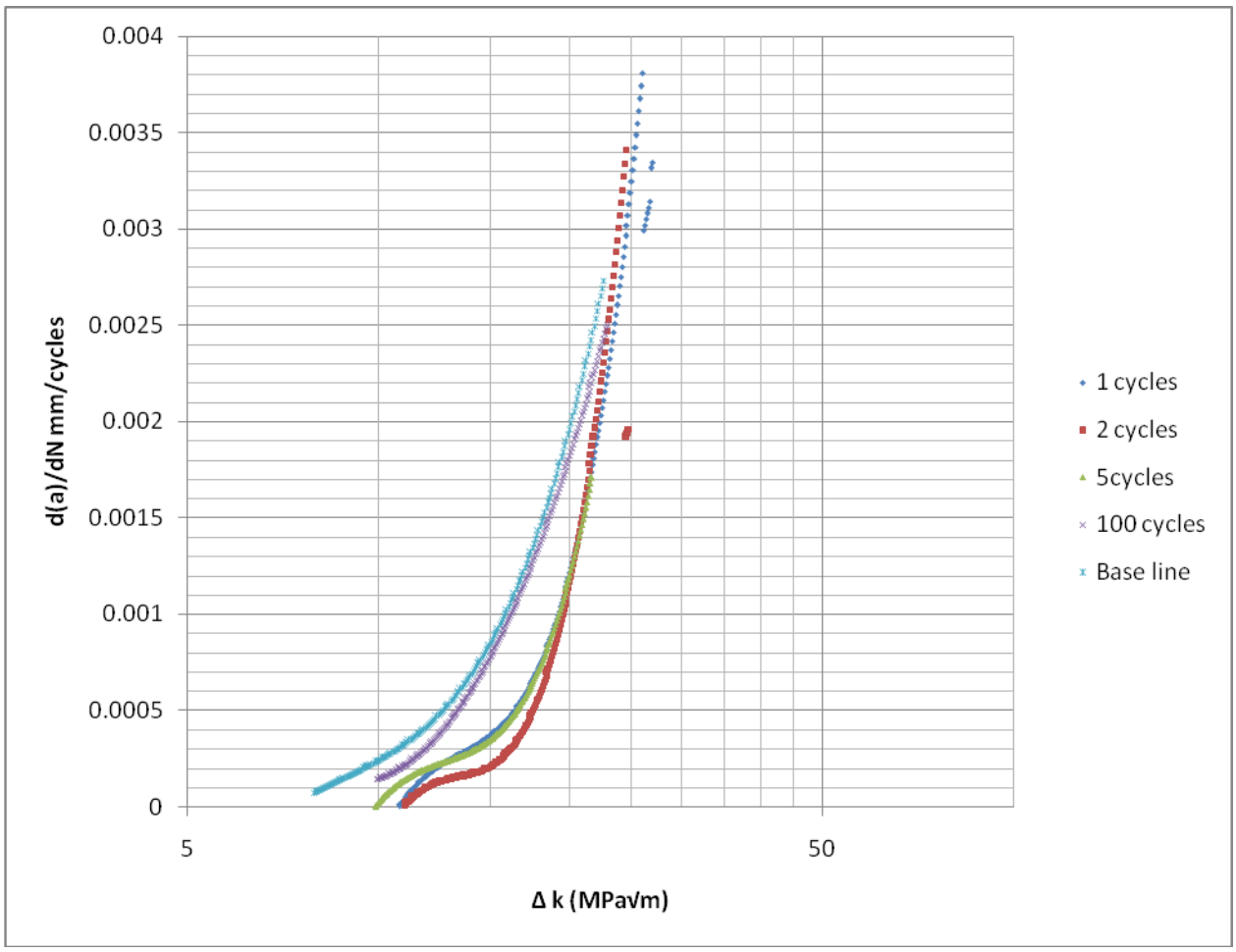

Figure 4.2 (a) Δ k vs da/dN curves for different overload cycles on semi-log scale

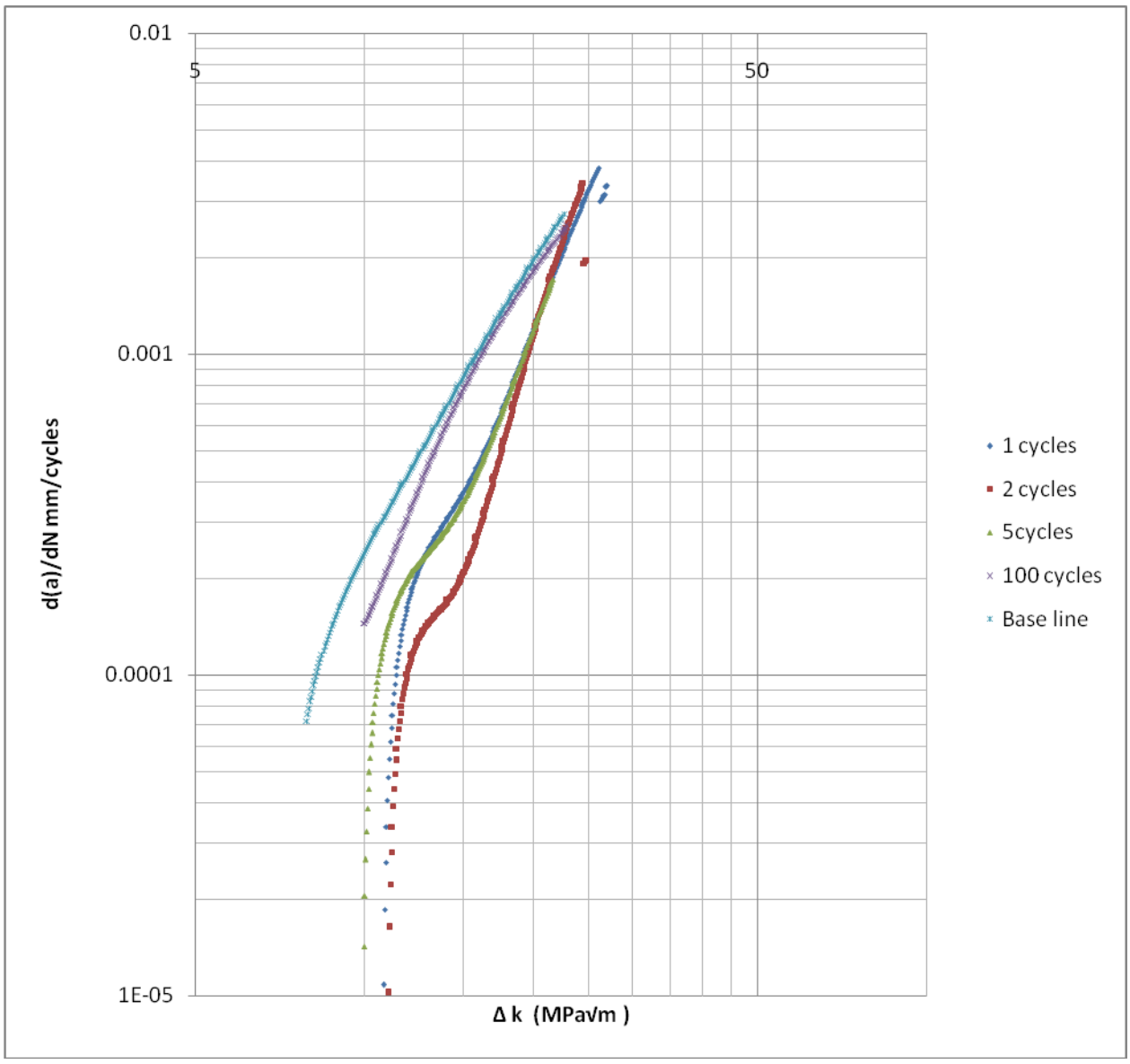

Figure 4.2 (b) Δ k vs da/dN curves for different overload cycles (log scale)

4.2 Fractogrpahy :

The fractured surfaces of the test specimens were examined under SEM and presented in following Figures(4.3-4.11). Fractogrpah of the specimen in the pre-overload region at *a*=19.12 mm and Δk=9.12 MPa√m has been presented in fig 4.3.

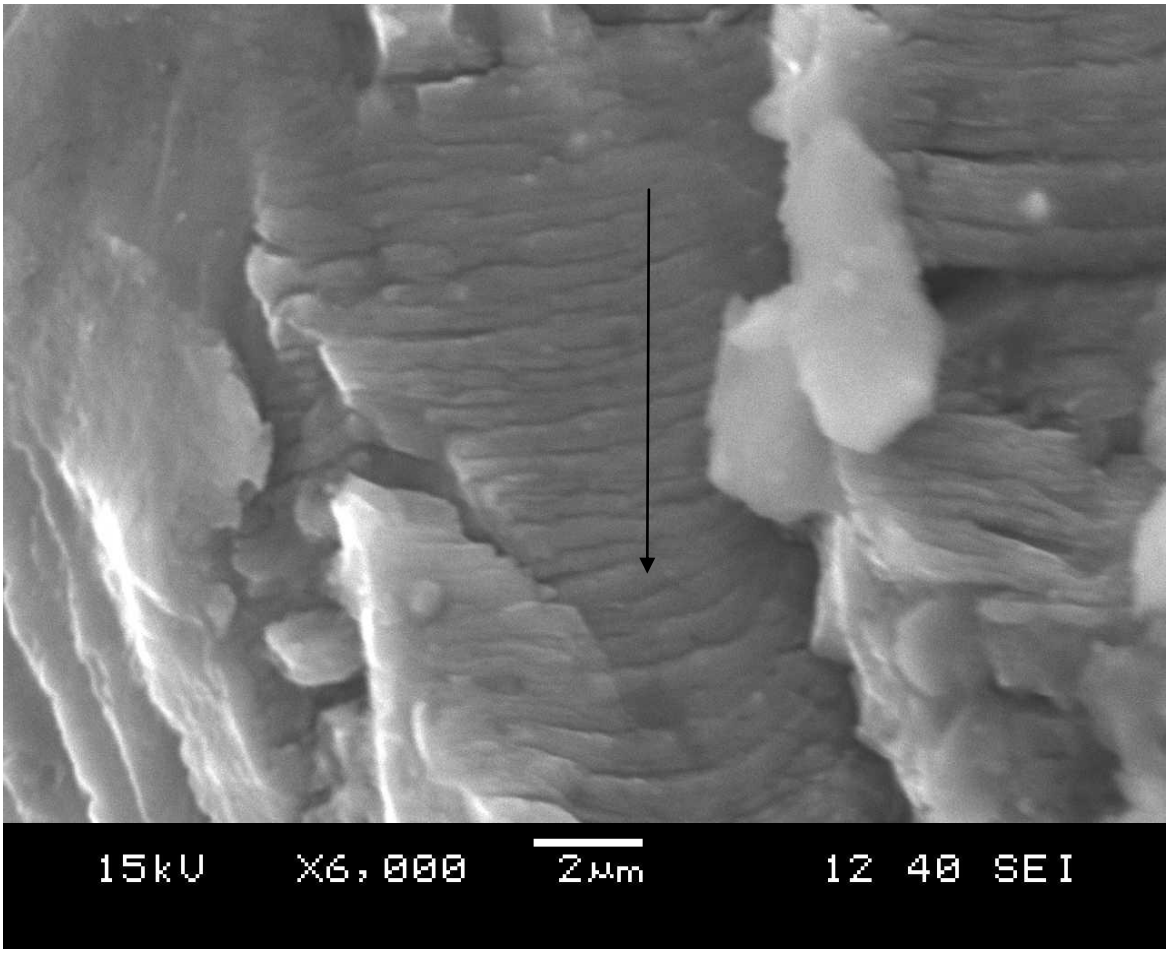

Figure 4.3 fracture surface at preoverloaded distance 19.12 mm distance for 2 overload cycles

The fractogrpah shows a transgranular fracture with well developed striation. The average width of striation in this zone is 0.48 µm .The corresponding measured fatigue crack growth rate is 1.71×10^{-05}. This suggests that the crack advancement does not occur cycle by cycle rather in an intermittent manner, a feature common in Al-alloy at low Δ*K*.

The fractograph of specimen just before application of overload cycles is illustrated in Fig 4.4 This also shows a well developed transgrannular striation.

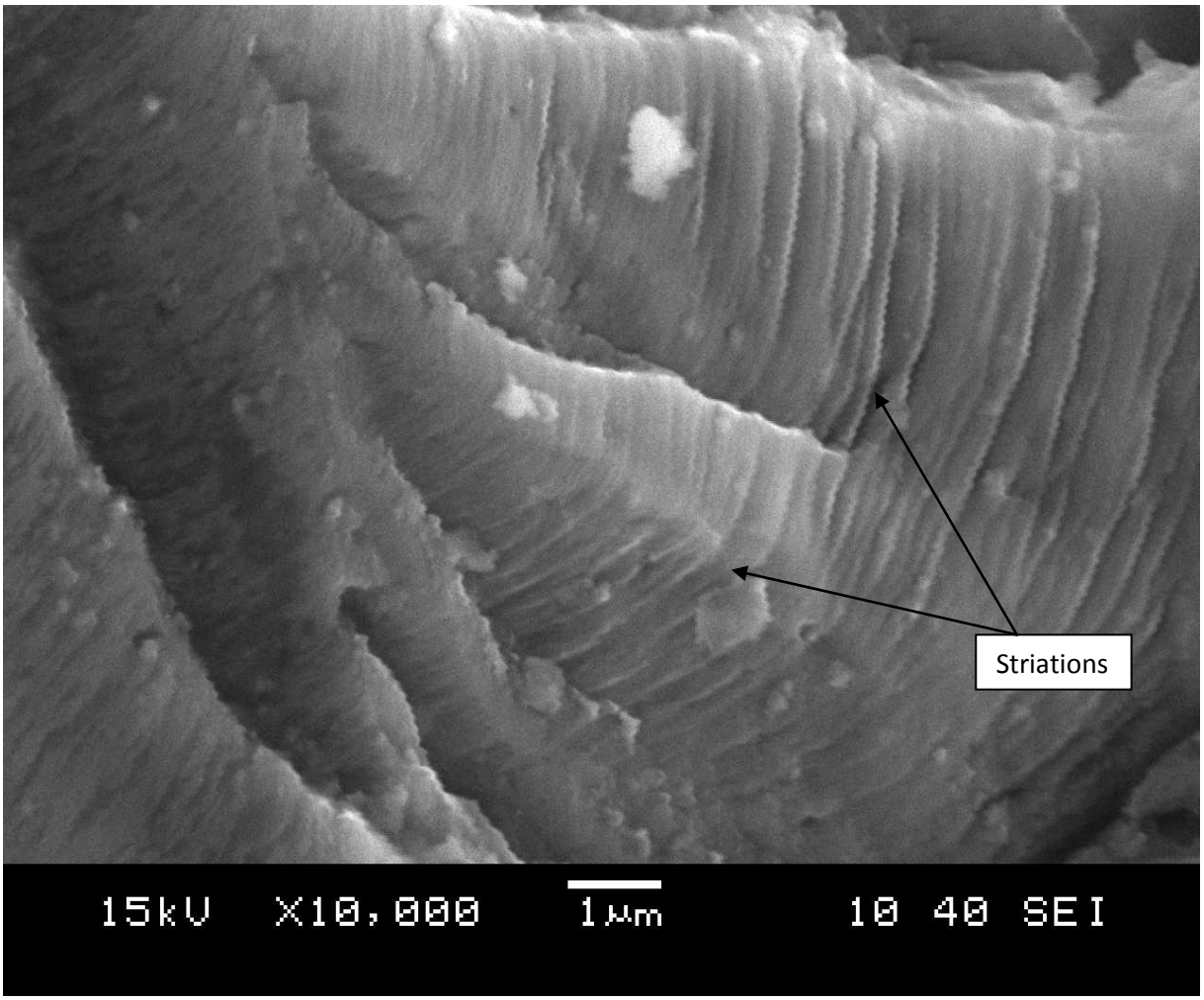

Figure.4.4 fractured surface just above the overload point for the specimen with overload 10 cycles

Fig.4.5 shows the fractogrpah at the point of overload application. The difference in the wide striation during overload application can be visualized in this figure. It is also worth to note that the striation developed during overload application do not remain confined to single grain and is intergrannular in nature. This is due to high SIF during overload application at ΔK=19 MPa$\sqrt{m}$.

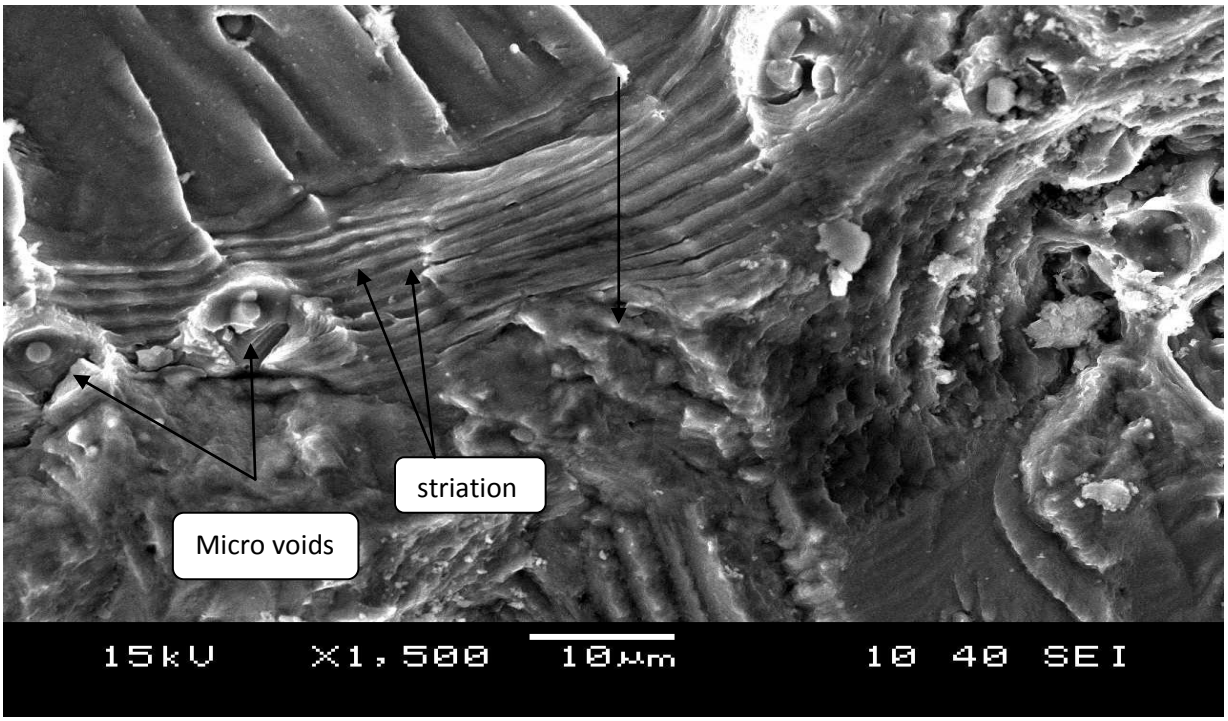

Figure 4.5 (a)

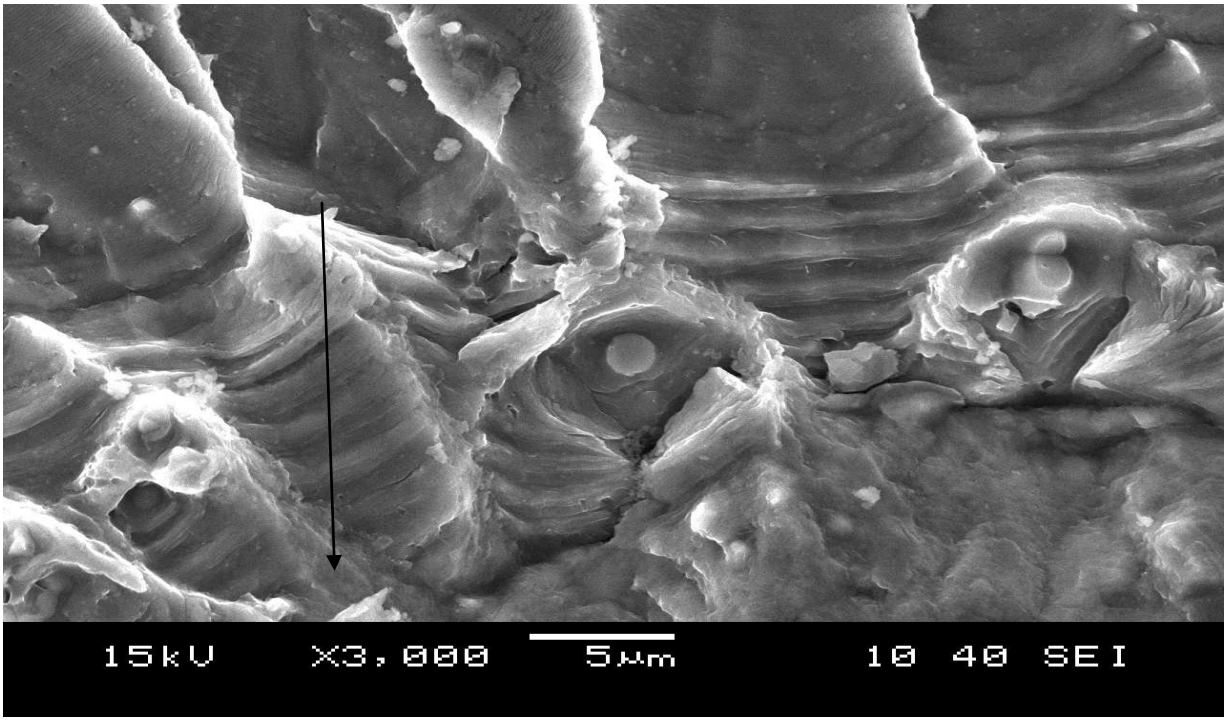

Figure.4.5-(b) crack growth at Tear zone for 10 overloaded cycles

This wide striation band formation has been followed by rough fracture zone. Striations are not visualized and this may be due to development of highly strain zone ahead of the crack tip on overload application. The featureless appearance of fracture zone may have developed due to multi-slip systems crack extension. There are also some micro voids and secondary cracks in this zone. This further suggests the development of highly strained zone on application of overload cycles. In case of 100 overload cycles application the feature is almost similar to the earlier specimen. There are also some micro voids and secondary cracks. It may be recalled that the extent of retardation reduces on application of multiple overload cycles figure (4.6).the overload tear zones are measured in different cases and presented in figure (4.4 and 4.8).The effect of overload cycles on width of tear zone is presented in figure (4.9).The width of the tear zones are nearly same for specimens subjected to overload cycles 2, 5 and 10.The appraisal increased in the tear zone is only notice in case of specimen subjected to 100 overload cycles. This suggests significant stress relaxation on application of large number of overload cycles. The reduction in magnitude of retardation in case of multiple overloading may be due to stress relaxation and it becomes very significant on inducing 100 cycles of overload.

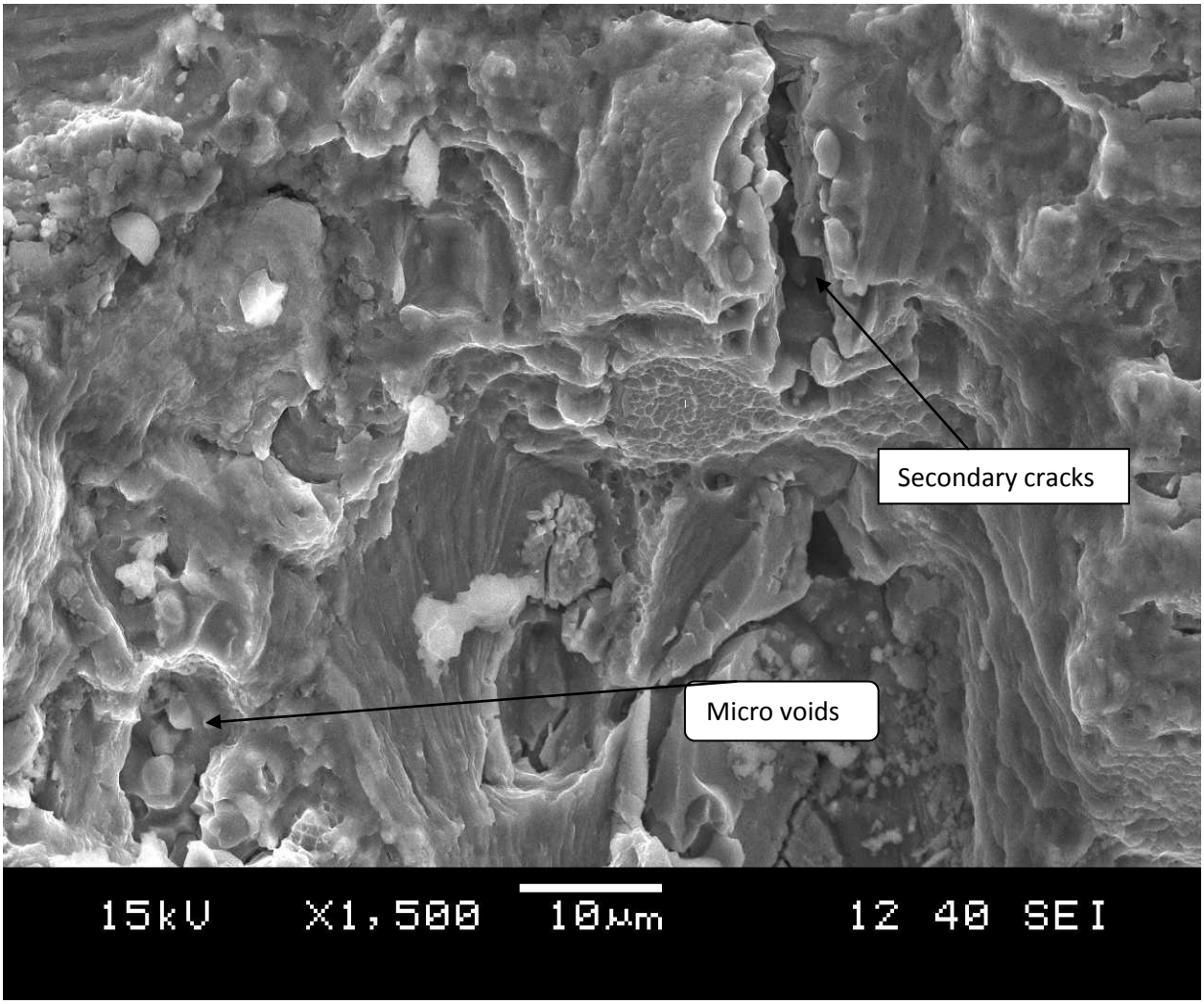

Figure 4.6 fractogrpah at overloaded zone for 100 overloaded cycles

.

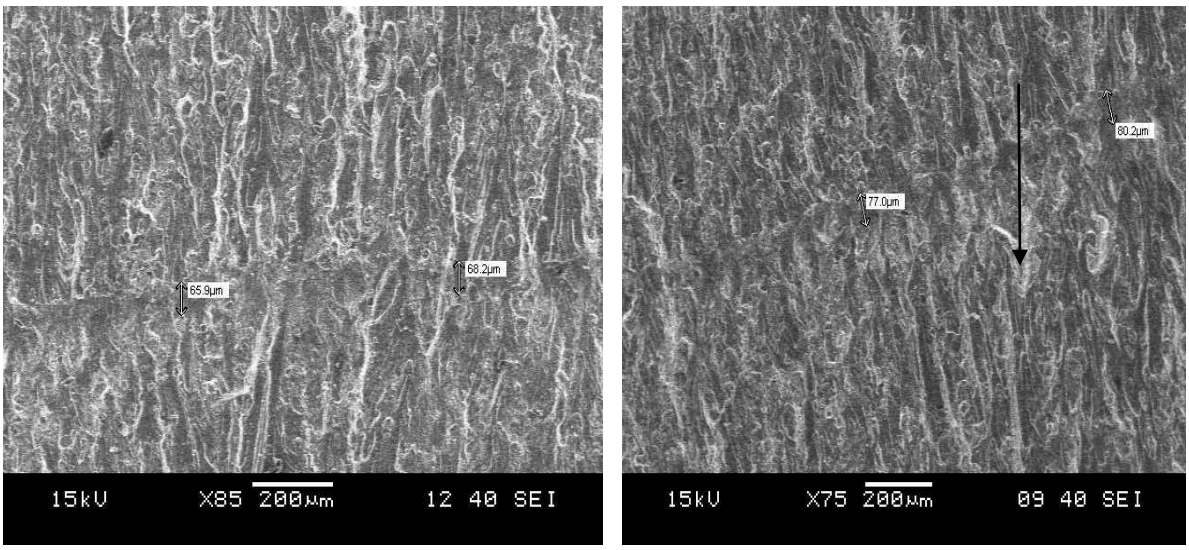

Figure 4.7 fractogrpah at overloaded zone for 2 and 10 overloaded cycles

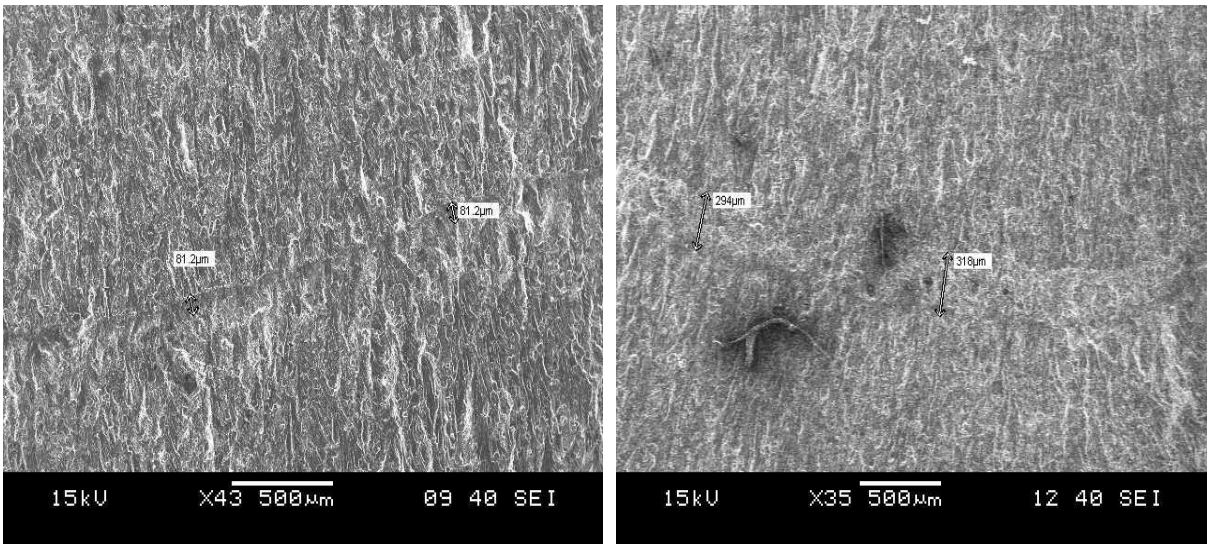

Figure 4.8 fractogrpah at overloaded zone for 5 and 100 overloaded cycles

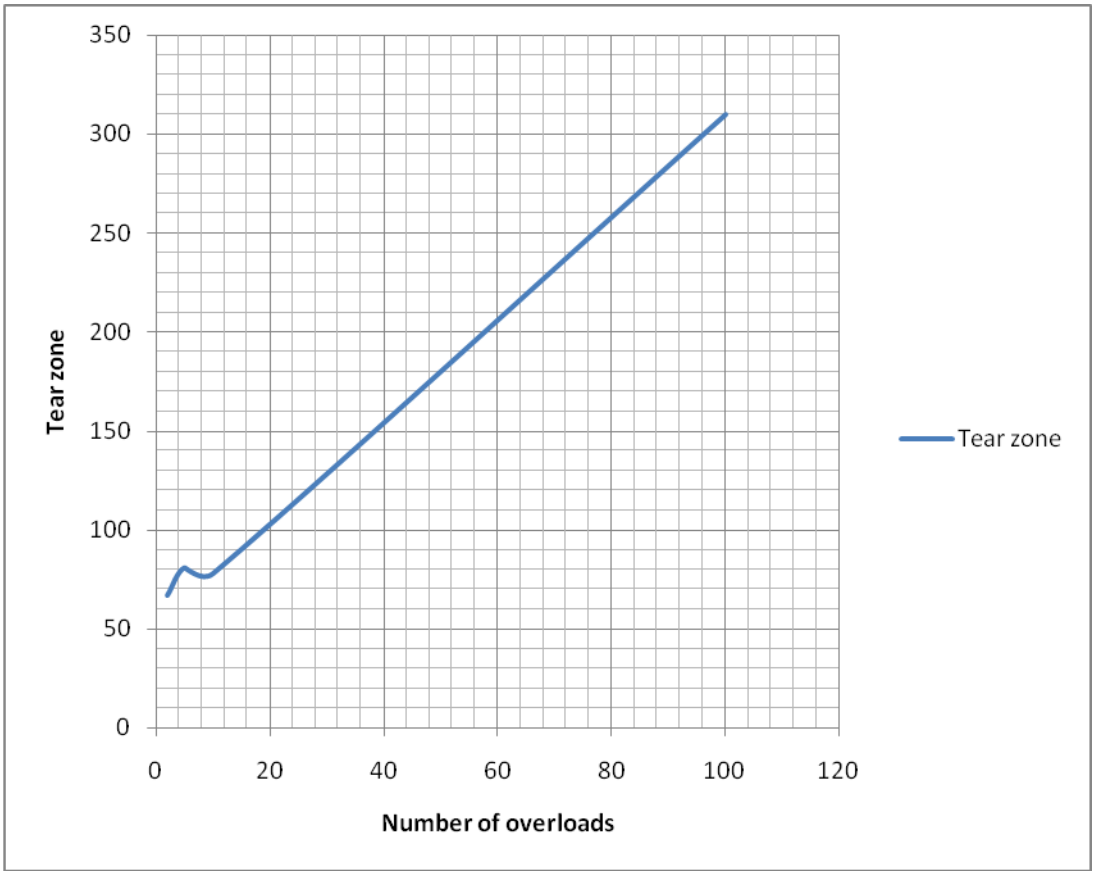

Figure 4.9 Graph for different overloaded cycles

Different values of tear zone and it's fractogrpah is shown in following figures and graph is shown in figure (4.9). From these figures it is clear that incase of 100 cycles band width is more may be due to stress relaxation, however it requires thorough analysis.

The fractography of post overloaded region of specimen subjected to 5 overload cycles and 100 overloaded cycles at a crack length *a*=21.5 mm are presented in figure8 and 9 respectively.

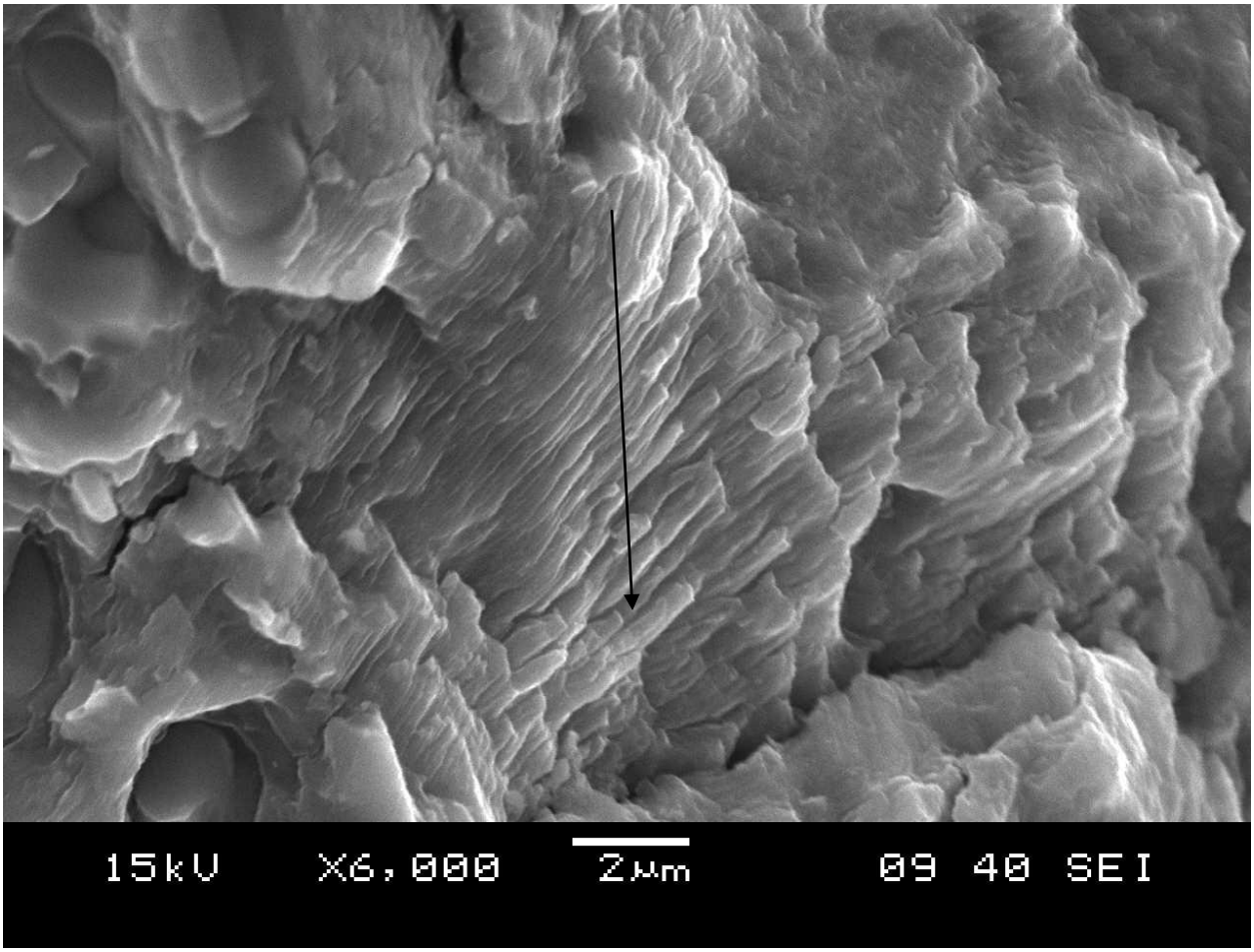

Figure 4.10 fractured surface in the post overload zone for 5 overload cycles

The differences in the crack growth rate are quite distinct. The average width of single striation in figure (4.8) is 0.22µm Where it is relatively large incase of overload 100 cycles is 0.67 µm. It is also important to note that crack extension in specimens experiencing ≤ 10 overload cycles it appears to be in highly strained region. On the other hand, the post overload crack extension appears to be ductile and a region free from the

pre-stresses. This also suggests a possibility of stress relaxation on application of large no of overload cycles. However this need to be verified and the minimum number of cycles required to relax the stresses to be identified.

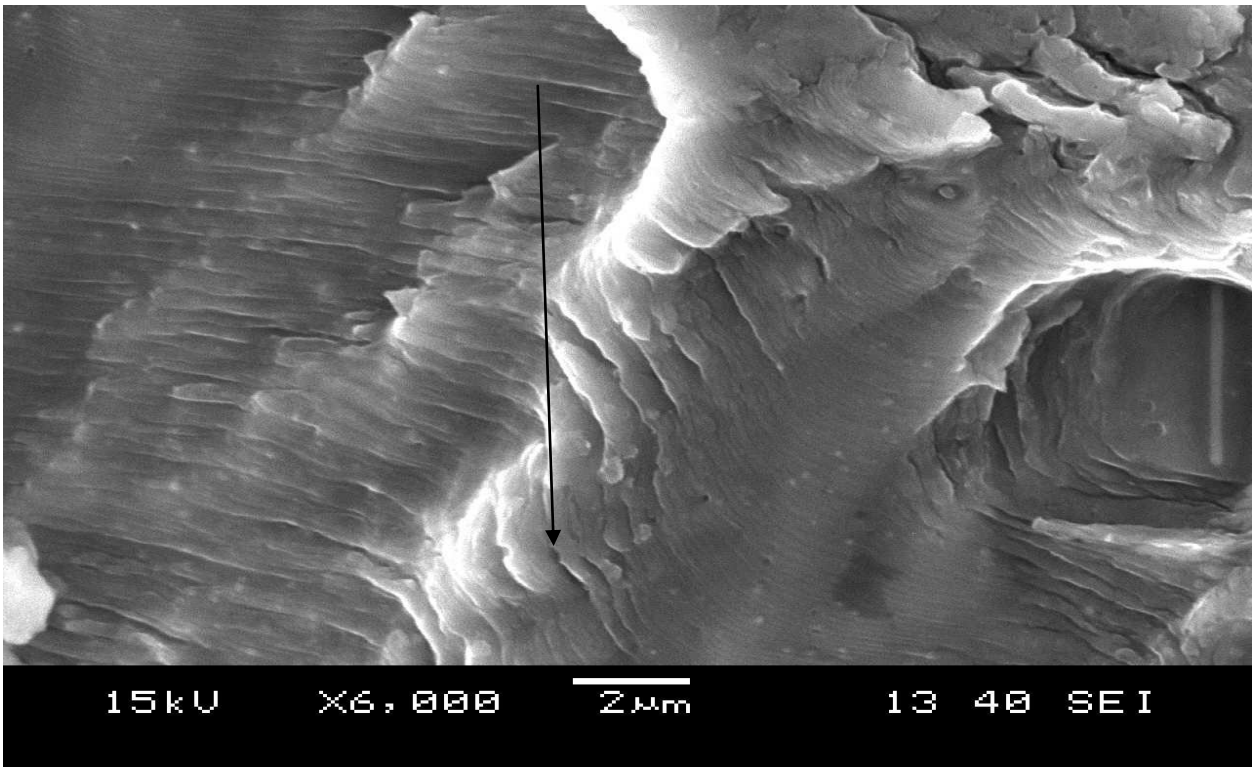

Figure 4.11 fractured surface in the post overload zone for 100 overload cycles

The specimen subjected to 100 overload cycles showing striations are ductile in nature in figure above figure (4.11). The observations are indirect evidence of the strain field ahead of the post overload zone. The specimen subjected to overloaded cycles less than 100 are highly strained. On the other hand there is stress retardation when specimen is subjected to 100 overload cycles. However it can be confined by measuring strain state ahead of the crack tip.

Chapter -5

5.1 Introduction of Modelling:

The prediction of life is certainly a challenging job for the engineering community because of two reasons. Firstly it is quite difficult to handle the robust integration scheme; secondly no single universal method is available as far as the different load interaction mechanisms are concerned .So adopted a new method called "Exponential Model" for life prediction under variable amplitude loading (spike overload).

Exponential model is associated with the name of Thomas Robert Malthus (1766-1834) who first realized that any species can potentially increase in numbers according to a geometric series. For example, if a species has non-overlapping populations (e.g., annual plants), and each organism produces R offspring, then, population numbers N in generations t=0,1,2,... is equal to:

$$N_1 = N_0 \cdot R$$
$$N_t = N_0 \cdot R^t$$

When t is large, then this equation can be approximated by an exponential function:

$$N_t = N_0 \cdot \exp(r \cdot t) = N_0 \cdot e^{rt} \tag{5.1}$$

There are 3 possible model outcomes:

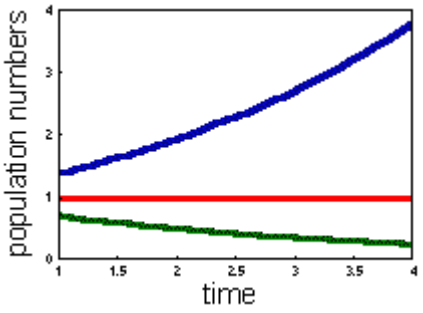

Figure 5.1 Model

1. Population exponentially declines ($r < 0$)
2. Population exponentially increases ($r > 0$)

3. Population does not change (r = 0)

Parameter r is called:

- Malthusian parameter
- Intrinsic rate of increase
- Instantaneous rate of natural increase
- Population growth rate

"Instantaneous rate of natural increase" and "Population growth rate" are generic terms because they do not imply any relationship to population density. It is better to use the term "Intrinsic rate of increase" for parameter r in the logistic model rather than in the exponential model because in the logistic model, r equals to the population growth rate at very low density (no environmental resistance).

Assumptions of Exponential Model:

1. Continuous reproduction (e.g., no seasonality)
2. All organisms are identical (e.g., no age structure)
3. Environment is constant in space and time (e.g., resources are unlimited)

However, exponential model is robust; it gives reasonable precision even if these conditions do not meet. Organisms may differ in their age, survival, and mortality. But the population consists of a large number of organisms, and thus their birth and death rates are averaged.

Parameter r in the exponential model can be interpreted as a difference between the birth (reproduction) rate and the death rate: $$\frac{dN}{dt} = (b - m)N = rN \qquad (5.2)$$

Where *b* is the birth rate and *m* is the death rate. Birth rate is the number of offspring organisms produced per one existing organism in the population per unit time. Death rate is the probability of dying per one organism. The rate of population growth (*r*) is equal to birth rate (*b*) minus death rate *(m*).

5.2 **Description of model:**

As mentioned in previous topic, differential equation for describing the exponential model is given by $\frac{dN}{dt} = \mathrm{rN}$

Where N is population and t is time.

The solution for above differential equation is given by $N(t) = N_0.e^{rt}$ (5.3).

However, in the present case, a crack will grow infinitely (of course the plate width has to be infinite) as $t \to \infty$. Therefore, equation (4) is modified and re-written as:

$$a_j = a_i e^{m_{ij}(N_j - N_i)} \tag{5.4}$$

$$m_{ij} = \frac{\ln\left(\frac{a_j}{a_i}\right)}{(N_j - N_i)} \tag{5.5}$$

where, a_i and a_j = crack length in i^{th} step and j^{th} step in 'mm' respectively,

N_i and N_j = No. of cycles in i^{th} step and j^{th} step respectively,

m_{ij} = specific growth rate in the interval *i*-j,

i = No. of experimental steps,

and $j = i+1$

The values of *m* can be calculated from crack extension and number of load cycles data. The important parameter in the model is the specific growth rate '*m*'.

Crack growth in a step can be influenced by maximum stress intensity factor occurring in a cycle K_{max}, background stress intensity factor ΔK, stress intensity factor at the time of application of overload K_{ol}, and on material properties like fracture toughness (in present

case plane strain fracture toughness K_c is considered), yield strength σ_x of material and modulus of elasticity E.

So, specific crack growth rate can be expressed as a function of dimension less quantities in terms of above mentioned parameters. [62]

$$\mathrm{m} = f\left(\left(\left(\frac{K_{max}}{\Delta K}\right)\left(\frac{K_C}{\Delta K}\right)\left(\frac{\sigma_{ys}}{E}\right)\right)^q\right) \tag{5.6}$$

or above equation can be simplified as

$$m = f(l)$$

Where

$$l = \left(\left(\frac{K_{max}}{\Delta K}\right)\left(\frac{K_C}{\Delta K}\right)\left(\frac{\sigma_{ys}}{E}\right)\right)^q \tag{5.7}$$

So in present model cubic polynomial is used to predict the values of m for different values of l.

Let $m = A'l^3 + B'l^2 + C'l + D'$ (5.8)

be the cubic polynomial

where, $l = \left[\left(\frac{\Delta K}{K_C}\right)\left(\frac{K_{max}}{K_C}\right)\left(\frac{\sigma_{ys}}{E}\right)\right]^{\frac{1}{4T}}$ (5.9)

and A', B', C', D' are material constants and T is No. of overload cycles.

The different '*m'* and '*l*' values are fitted by 3rd degree polynomial of post overload portion. The predicted '*m'* values are calculated as per equation

Since the above constants are different for each overloaded cycles, In order to find material constant at any 10 overloaded cycles a log curve has fitted between a set of material constants and their corresponding overloaded value.

Overload cycles	A’	B’	C’	D’
1	1E-07	8 E-06	0	0.001
2	21680	-65258	6600	-223.6
5	10444	-19684	12369	25914
100	-1E+07	-4E-07	4E+07	1E+07
Predicted values for 10	-4 E+06	-1.6 E-07	24570	82500

Table 5.1 different values of constant A’ ,B’ ,C’ and D’

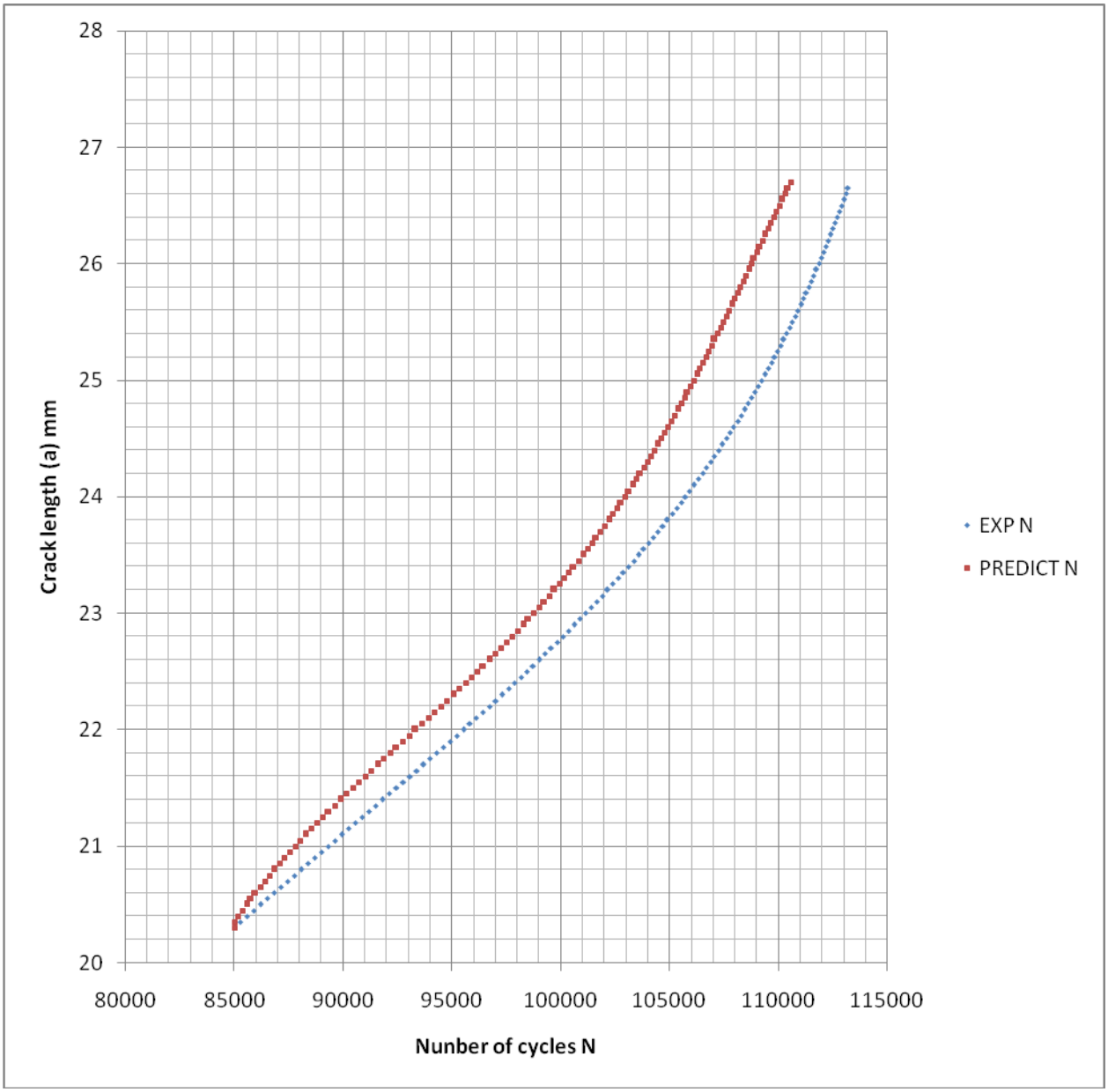

Figure 5.2 No of cycles~ crack length m (mm)

Chapter -6

Conclusions

6.1 **Conclusions:**

1. The overload application reduces the crack growth rate and results in enhanced fatigue life.
2. The overload application for a single cycle gives the maximum retardation and longer fatigue life as compared to 2, 5, 10 and 100 cycles.
3. This enhanced retardation effect is explained on the basis of large number of secondary cracks formed in the overload tear zone. These secondary cracks reduce available ΔK for the crack extension.
4. An exponential model fits well and can be used to predict post overload life of a component.

References

1. Fatigue of Materials S.Suresh 2nd edition Cambridge university press November 28 1999.
2. Ali Merati A study of nucleation and fatigue behavior of an aerospace aluminum alloy 2024-T3; International Journal of Fatigue 27 (2005) 33–44
3. Muskhelishvli, N.I., Some basic problems of mathematical theory of elasticity. Tata McGraw Hill publication.
4. Larid C, (1967), Influence of metallurgical structure on Mechanisms of fatigue crack propagation. Int J Fatigue 1998;21:S283–46.
5. Irwin, G.R, (1957), Analysis of stresses and strains near the end of a crack traversing a plate. Journal of Applied Mechanics 24, 361-4.
6. Sadananda K, Vasudevan AK, et al. Analysis of fatgue crack closure and threshold Int J Fatigue 1999;21:S233–46
7. Wells AA., Application of fracture mechanics at and beyond general yield, British Welding Res. Ass. Rept., M13/63 (1963).
8. Elber, W., 'The significance of fatigue closure', Damage Tolerance In Aircraft Structures, ASTM STP 486, American Society of Testing and Materials, 1971, pp. 230-242
9. Halliday & Beevers (1981) Some aspects of crack closure in two contrasting Al alloys; Journal of testing and evaluation, vol 9, 192-201.
10. Liaw P.K, Leax T.R. & Logsdon W A. (1983) Near threshold fatigue crack growth behavior in metals Acta Metallurgica 31, 1581-87.
11. Kim. J.H, Lee. S.B. Behavior of plasticity-induced crack closure and roughness-induced crack closure in aluminum alloy, International Journal of Fatigue 23 (2001) S247–S251
12. Lam YC, Griffiths JR, Effect of increment heating on fatigue crack growth, Theoretical applied fracture mechanics 1990;14;37-41.
13. Harison JD. Br Weld J 1965;12:258.

14. P.K Ray, B.B Verma, Spot heating induced fatigue crack retardation, Int J of Press vessels and piping 79; 2002;373-376.
15. Ward-Close CM, Blom AF, Ritchie RO. Mechanisms associated with transient fatigue crack growth under variable-amplitude loading: an experimental and numerical study. Engineering Fracture Mechanics 1989;32:613–38.
16. Luiz Fernando Martha; Evaluation of crack growth retardation in branched fatigue cracks Marco Antonio Meggiolaro 1 Antonio Carlos de Oliveira Miranda,Jaime Tupiassú Pinho de Castr,
17. McEvily AJ, Ishikawa S, Makabe C. The influence of the baseline R value on the extent of retardation after an overload. Mechanism and mechanics of fracture. The John Knott Symposium, TMS, 2002. p. 37–42.
18. Verma. B.B, Ashok Kumar and Ray. P.K.; Fatigue crack growth delay following overload, trans. indian inst. met. vo1.53, no.6, December 2000, pp. 591-595
19. Willenborg JD, Engle RM, Wood HA. A crack growth retardation model using an effective stress concept, Report AFFEL-TM-71-1- FBR, Dayton (OH): Air Force Flight Dynamics Laboratory, Wright– Patterson Air Force Base; 1971.
20. NASA, Fatigue crack growth computer program "NASGRO", Version 3.0 – Reference manual, 2000.
21. Wheeler OE. Spectrum loading and crack growth. J Basic Eng Trans ASME Series D 1972;94:181–6.
22. Aliaga D, Davy A, Schaff. H. Mechanics of Fatigue Crack Closure, edited by Newman Jr JC 1987. p. 491-504.
23. Padmadinata UH. Investigation of crack-closure prediction models for fatigue in aluminium alloy sheet under flight-simulation loading, PhD-thesis, Delft 1990.
24. Baudin G, Labourdette R, Robert M. In Fatigue crack growth under variable amplitude loading, edited by Petit J et al. Elsevier Applied Science, London 1988. p. 292-308.
25. De Koning AU. A simple crack closure model for prediction of fatigue crack growth rates under variable-amplitude loading. In: Roberts Richard, editor. Fracture mechanics: thirteenth conference. ASTM STP, vol. 743. American Society for Testing and Materials; 1981. p. 63–85.

26. Newman Jr JC. A crack-closure model for predicting fatigue crack growth under aircraft spectrum loading. In: Chang JB, Hudson CM, editors. Methods and models for predicting fatigue crack growth under random loading. ASTM STP, vol. 748. American Society for Testing and Materials; 1981. p. 53–84.
27. De Koning AU, van der Linden HH. Prediction of fatigue crack growth rates under variable loading using a simple crack closure model. NLR MP 81023U, Amsterdam 1981.
28. Pompetzki MA, Topper TH, Duquesnay DL, Yu MT. Effect of compressive and tensile overloads on fatigue damage accumulation in 2024-T351 aluminum. J Testing Evaluat 1990;18(1): 53–61.
29. Murthy ARC, Palani GS and Iyer NR. State-of-the-art review on fatigue crack growth analysis under variable amplitude loading. IE (I) Journal-CV 2004;85:118-29.
30. Newman Jr JC. Effects of constraint on crack growth under aircraft spectrum loading. In: Beukers A, editor. Fatigue of aircraft materials: Delft University Press; 1992. p. 83–109.
31. Zapatero J,Moreno B, Dominguez J.On the use of the strip-yield model to predict fatigue crack growth under irregular loading. Fatigue Fract Eng Mater Struct 1997;20(5):759–70.
32. Harter JA.Comparison of contemporary FCG life prediction tools. Int J Fatigue 1999;21:S181–S5.
33. Bunch JO, Tammell RT, Tanouye PA.Structural life analysis methods used on the B-2 bomber. In: Mitchell MR, Landgraf RF, editors. ASTM STP 1292. American Society for Testing and Materials; 1996.p. 220–47
34. C. M. Ward-Close and R. O. Ritchie, On the role of crack closure mechanisms in influencing fatigue crack growth following tensile overloads in a titanium alloy: near threshold versus higher AK behavior. ASTM STP 982, 93-111 (1988)
35. S. Suresh, Micromechanisms of fatigue crack growth retardation following overloads. Engng Fracture Mech. 18, 577-593 (1983).
36. Petit. J., Tintillier. R., Ranganathan. N., Abdedaim. M. Ait and Chalant. G., Influence of microstructure and environment on fatigue crack propagation affected by single or repeated overloads in 7075 alloy, in Fatigue Crack Growth Under Variable Amplitude Loading (Edited by J. Petit, D, L. Davidson, S. Suresh and P. Rabbe), pp. 162-179. Elsevier Applied Science (1988).

37. Blom. A. F., Spectrum fatigue crack growth, in Fatigue Crack Growth Under Variable Amplitude Loading (Edited by J. Petit, D. L. Davidson, S. Suresh and P. Rabbe), pp. 231-250. Elsevier Applied Science (1988).
38. Shin. C. S. and Hsu. S. H, On the mechanisms and behavior of overload retardation in AISI 304 stainless steel. Int. J. Fatigue 15, 181-192 (1993).
39. Zuidema. J., Mense. P. J. M and R. A. H. Edwards, Environmental dependence of fatigue crack growth retardation following a single overload in 2024-al alloy. Engng Fracture Mech. 26, 927 935 (1987).
40. Chert. D. and Nisitani. H., Analysis of the delaying effects of overloads on fatigue crack propagation. Engng Fracture Mech. 39, 287-298 (1991).
41. Damri D.and Knott. J. F., Transient retardations in fatigue crack growth following a single peak overload. Fatigue Fracture Engng Mater.Structures 14, 709-719 (1991).
42. Skorupa. M. Experimental results and predictions on fatigue crack growth in structural steel Fatigue & Fracture of Engineering Materials & Structures Int J Fatigue Vol. 22 (1999), p. 905.
43. Schijve. J. ΔK_{eff} parameter under re-examination▪Fatigue & Fracture of Engineering Materials & Structures Int J Fatigue Vol. 22 (1999), p. 87
44. Paris PC, Tada H, Donald JK. Service load fatigue damage – a historical perspective. Int J Fatigue 1999;21:S35–46.
45. Sadananda K, Vasudevan AK, et al. Analysis of overload effects and related phenomena. Int J Fatigue 1999;21:S233–46.
46. James MN, Paterson AE. Fatigue performance of 6261-T6 aluminium alloy – constant and variable amplitude loading of parent plate and welded specimens. Int J Fatigue 1997;19:S109 18.
47. Taheri F, Trask D, Pegg N. Experimental and analytical investigation of fatigue characteristics of 350WT steel under constant and variable amplitude loading. Mar Struct 2003;16:69–91.
48. Wheeler OE. Spectrum loading and crack growth. J Basic Engng, Trans ASME, Ser D 1972;94(1):181–6.
49. Willenborg JD, Engle Jr RM, Wood HA. A crack growth retardation model using effective stress concept. AFDL-TM-71-1-FBR. January 1971.

50. Elber W. The significance of fatigue crack closure in fatigue. ASTM STP 1972;486:230–42.
51. Newman Jr JC. A crack opening stress equation for fatigue crack growth. Int J Fract 1984;24:R131–5.
52. Ray A, Patanker P. Fatigue crack growth under variable amplitude loading: Part I – Model formulation in state space setting. Appl Math Model 2001;25:979–94.
53. Ray A, Patanker R. Fatigue crack growth under variable-amplitude loading: Part II-Code development and model validation. Appl Math Model 2001;25:995–1013.
54. Newman Jr JC. Phillips EP, Everett RA. Fatigue analyses under constant and variable amplitude loading using small-crack theory. NASA/TM-1999-209329, ARL-TR-2001.
55. Schijve J. Some formulas for the crack opening stress level. Engng Fract Mech 1981;14:461–5.
56. Voorwald HJC, Torres MAS. Modeling of fatigue crack growth following overloads. Int J Fatigue 1991;13(5):423–7.
57. Huang XP, Cui WC, Leng JX. A model of fatigue crack growth under various load spectra. In: Proc of Sih GC, 7th Int conf of MESO, August 1–4, Montreal, Canada; 2005. p. 303–08.
58. Huang XP, Zhang JB, Cui WC, Leng JX. Fatigue crack growth with overload under spectrum loading. Theor Appl Fract Mech 2005;44:105–15.
59. Raghuvir Kumar & S. B. L. Garg. Effect of Periodic Bands of Overloads on Crack Closure Int. J. Pres. Ves. & Piping 38 (1989) 27-3
60. Brown WF, Srawley JE.Plane strain crack toughness testing of high strength metallic materials. ASTM STP, ASTM, Philadelphia, USA, vol. 410. 1966. p. 1.
61. J.R.Mohanty.J.R, Ray.P.K, Verma.B.B Evaluation of overload-induced fatigue crack growth retardation parameters using an exponential model Engineering Fracture Mechanics Volume 76
62. J.R Mohanty. J.R, Ray. P.K, Verma. B.B Prediction of fatigue life with interspersed mode-I and mixed-mode (I and II) overloads by an exponential model: Extensions and improvements Engineering Fracture Mechanics Volume 76, Issue 3, February 2009, Pages 454-468
63. Mohanty.J.R, Ray. P.K, Verma. B.B Prediction of fatigue crack growth and residual life using an exponential model: Part II (mode-I overload induced retardation) Int J of Fatigue Volume 31, Issue 3, March 2009, Pages 425-432